1

2

Title

Stimulation of the catalytic activity of the tyrosine kinase Btk by the adaptor protein Grb2

5

Authors

Laura M. Nocka[a,b,c,d], Jay T. Groves[a,b,e], John Kuriyan[a,b,c,f]

8

[a] Department of Chemistry, University of California, Berkeley, CA 94720

[b] California Institute for Quantitative Biosciences, University of California, Berkeley, CA 94720

[c] Howard Hughes Medical Institute, University of California, Berkeley, CA 94720

[d] Current affiliation: Department of Biochemistry, Stanford University, Stanford, CA 94305

[e] Institute for Digital Molecular Analytics and Science, Nanyang Technological University, 639798 Singapore

[f] Department of Molecular and Cell Biology, University of California, Berkeley, CA 94720

16

For correspondence: kuriyan@berkeley.edu or jtgroves@lbl.gov

18

Abstract

The Tec-family kinase Btk contains a lipid-binding Pleckstrin homology and Tec homology (PH-TH) module connected by a proline-rich linker to a "Src module", an SH2-SH3-kinase unit also found in Src-family kinases and Abl. We showed previously that Btk is activated by PH-TH dimerization, which is triggered on membranes by the phosphatidyl inositol phosphate PIP_3, or in solution by hexakisinositol phosphate (IP_6) (Wang *et al.* 2015, https://doi.org/10.7554/eLife.06074). We now report that the ubiquitous adaptor protein growth-factor-receptor-bound protein 2 (Grb2) binds to and substantially increases the activity of PIP_3-bound Btk on membranes. Using reconstitution on supported-lipid bilayers, we find that Grb2 can be recruited to membrane-bound Btk through interaction with the proline-rich linker in Btk. This interaction requires intact Grb2, containing both SH3 domains and the SH2 domain, but does not require that the SH2 domain be able to bind phosphorylated tyrosine residues – thus Grb2 bound to Btk is free to interact with scaffold proteins via the SH2 domain. We show that the Grb2-Btk interaction recruits Btk to scaffold-mediated signaling clusters in reconstituted membranes. Our findings indicate that PIP_3-mediated dimerization of Btk does not fully activate Btk, and that Btk adopts an autoinhibited state at the membrane that is released by Grb2.

Introduction

B cell signaling relies on the sequential activation of three tyrosine kinases that transduce the stimulation of the B cell receptor (BCR) into the generation of calcium flux and the initiation of signaling pathways, such as the Ras/MAPK pathway (Engels, Engelke, & Wienands, 2008; Weiss & Littman, 1994). Activation of a Src-family kinase, Lyn, results in the phosphorylation of ITAMs (Immunoreceptor Tyrosine-based Activation Motifs) in the cytoplasmic tails of the B cell receptor. This results in the recruitment and activation of the tyrosine kinase Syk, which phosphorylates the scaffold protein SLP65 (SH2 domain-containing Leukocyte Protein of 65 kDa) also known as BLNK (B-cell Linker Protein) (Kurosaki & Tsukada, 2000). The activation of Syk triggers the recruitment of diverse signaling proteins to the plasma membrane, including the Tec-family kinase Btk, which is critical for the development and proliferation of mature B cells (Figure 1A) (Hendriks, Yuvaraj, & Kil, 2014; Rip, Van Der Ploeg, Hendriks, & Corneth, 2018; Scharenberg, Humphries, & Rawlings, 2007; Tsukada et al., 1993). Signaling by the T cell receptor follows a similar pathway, with the Src-family kinase Lck activating the Syk-family kinase Zap-70 (Zeta-chain-associated protein kinase of 70 kDa). Zap-70 phosphorylates the scaffold protein LAT (Linker for Activation of T cells), which leads to the activation of the Tec-family kinase Itk (Interleukin-2-inducible T cell Kinase) (Courtney, Lo, & Weiss, 2018; Weiss & Littman, 1994).

Btk has an N-terminal PH-TH module, consisting of a Pleckstrin-homology (PH) domain followed by a Zinc-bound Tec-homology (TH) domain. The PH-TH module is connected through a proline-rich linker to a Src module, comprising an SH3 domain, an SH2 domain, and a kinase domain (Figure 1B) (Joseph, Wales, Fulton, Engen, & Andreotti, 2017; Shah, Amacher, Nocka, & Kuriyan, 2018; Wang et al., 2015). The Src module of Btk is structurally similar to the corresponding modules of other cytoplasmic tyrosine kinases such as c-Src, Lck and Abl. SH2 domains bind to phosphotyrosine-containing peptides, while SH3 domains recognize specific PxxP motifs within proline-rich peptide segments. In the autoinhibited forms of kinases with Src modules, the SH3 domain and the N-terminal lobe of the kinase domain sandwich the SH2-

64 kinase linker, and the SH2 domain sits adjacent to the C-terminal lobe of the kinase domain.
65 Together these contacts prevent the kinase domain from adopting an active conformation
66 (Amatya, Lin, & Andreotti, 2019; Shah et al., 2018). The PH-TH module of Btk is connected to
67 the Src module by a 44-residue linker that contains ten proline residues and two PxxP motifs that
68 are potential SH3-binding sites. Btk is recruited to the membrane through binding of PIP_3 by the
69 PH-TH module (Baraldi et al., 1999; Chung et al., 2019; Hyvönen & Saraste, 1997).
70   Crystal structures of the Btk PH-TH module, first determined by the late Matte Saraste
71 and colleagues, reveal a dimeric arrangement, which we refer to as the "Saraste dimer" (Baraldi
72 et al., 1999; Hyvönen & Saraste, 1997). Mutagenesis of residues at the Saraste-dimer interface
73 has shown that the PH-TH dimer is critical for Btk activity in cells (Chung et al., 2019). Btk is
74 activated *in vitro* by vesicles containing PIP_3, or by inositol hexakisphosphate (IP_6) in solution
75 (Kim et al., 2019; Wang et al., 2015). The activation by IP_6 requires formation of the Saraste
76 dimer, and involves the binding of two IP_6 molecules, one bound at the canonical PIP-binding
77 site in the PH domain and the other to a peripheral site. The physiological relevance of the IP_6-
78 stimulated Btk activity in T cell-independent B cell activation has been demonstrated recently
79 (Kim et al., 2019). Experiments on supported-lipid bilayers, as well as molecular dynamics
80 simulations, have shown that PIP_3 in membranes promotes dimerization of the PH-TH module
81 through binding to the canonical and peripheral sites (Chung et al., 2019; Wang, Pechersky,
82 Sagawa, Pan, & Shaw, 2019).
83   Our understanding of the structure of Btk is based on structures determined separately for
84 the isolated PH-TH module, the Src module, and a construct in which the PH-TH module is
85 linked artificially to the kinase domain (Baraldi et al., 1999; Hyvönen & Saraste, 1997; Wang et
86 al., 2015). All four domains of Btk participate in maintaining the autoinhibited state (Figure 1B).
87 Deletion of the PH-TH domain from full-length Btk results in a more active kinase *in vitro*
88 (Wang et al., 2015). NMR analysis demonstrates that there is an autoinhibited form of Btk in
89 which the PH-TH module interacts with the kinase domain differently than observed in the
90 crystal structure of the PH-TH-kinase fusion, but the structure of this state remain to be defined
91 in detail (Joseph et al., 2017). Additionally through mutational studies and SAXS measurements
92 an SH2-kinase interface that stabilizes an active form of the Btk has been identified (Duarte et
93 al., 2020). Together these studies suggest a dynamic equilibrium between active and
94 autoinhibited forms of the kinase.
95   Adaptor proteins play critical roles in facilitating the organization of enzymes during
96 signal transduction (Hashimoto et al., 1999; Koretzky, Abtahian, & Silverman, 2006; Rodriguez
97 et al., 2001). Growth-factor-receptor-bound protein 2 (Grb2) is a ubiquitous adaptor protein that
98 is important for receptor tyrosine kinase signaling and the mitogen-activated protein kinase
99 (MAPK) pathway (Cantor, Shah, & Kuriyan, 2018; Clark, Stern, & Horvitz, 1992; Gale, Kaplan,
100 Lowenstein, Schlessinger, & Bar-Sagi, 1993; Lowenstein et al., 1992; Olivier et al., 1993). Grb2
101 consists of two SH3 domains that flank an SH2 domain (Figure 1C). Grb2 is responsible for
102 bringing signaling enzymes to their substrates and also helps in the formation of signaling
103 clusters at the plasma membrane by virtue of its ability to crosslink scaffold proteins or receptors
104 (Huang et al., 2019; Huang, Chiang, & Groves, 2017; Huang et al., 2016; C.-W. Lin et al., 2022;
105 Su et al., 2016). For example, in the MAPK pathway, the SH3 domains of two Grb2 molecules
106 bind to the Ras activator Son of Sevenless (SOS). Grb2 binds to scaffold proteins, such as SLP65
107 in B cells and LAT in T cells, through interaction of the Grb2 SH2 domain with phosphotyrosine
108 residues on the scaffold proteins (Engels et al., 2009; Reif, Buday, Downward, & Cantrell,
109 1994). In this way, Grb2 recruits SOS to the scaffold proteins or receptors, and the interaction of

110   one SOS molecule with two Grb2 molecules promotes crosslinking of these proteins. In T cells,
111   a protein closely related to Grb2, GADS (Grb2-related adaptor downstream of Shc), works
112   together with Grb2 to crosslink scaffolding proteins and enzymes downstream of the TCR (T cell
113   receptor) (Liu, Fang, Koretzky, & McGlade, 1999). Grb2 is also reported to be capable of
114   dimerization, and dimeric Grb2 hinders basal signaling of the fibroblast growth factor receptor 2
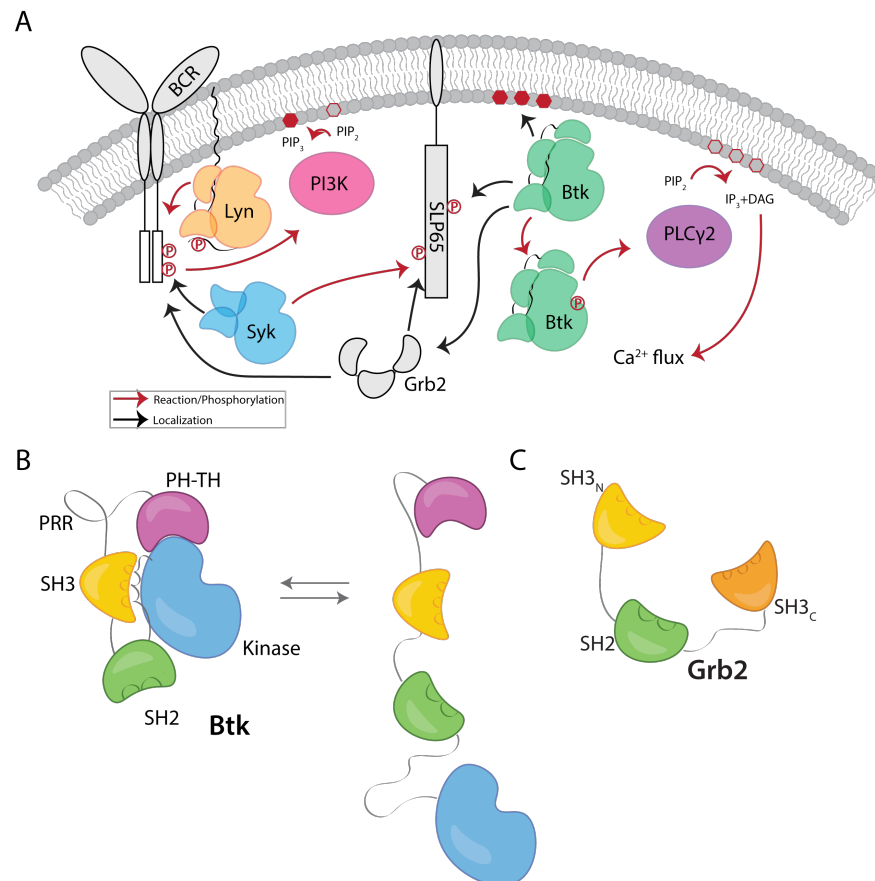115   (FGFR2), thereby tuning the activity of the receptor (C.-C. Lin et al., 2012).
116

117
118
119   **Figure 1. Btk and Grb2 are integral to B-cell signaling.** A) The B cell signaling cascade relies
120   on kinases and adaptor molecules. B) Btk is made up of five distinct domains. The Pleckstrin
121   homology and Tec homology domains fold together into one module (PH-TH), which is
122   connected through a linker containing two proline-rich regions (PRR) to the Src module (SH3,
123   SH2 and kinase domain). These domains together mediate autoinhibition of Btk. C) Grb2
124   domain architecture consists of two SH3 domains that flank an SH2 domain.
125
126   Memory-type B cells expressing membrane-bound IgG (mIgG) as a component of the
127   BCR rely on an immunoglobulin tail tyrosine (ITT) motif that is phosphorylated by Syk and
128   recruits Grb2 through binding of its SH2 domain to the resulting phosphotyrosine residues. It
129   was shown, by fusing domains of Grb2 to the IgG tail (in the absence of the ITT motif), that the
130   N-terminal SH3 domain of Grb2 plays a critical role in generating downstream signals. Affinity
131   purifications using the isolated N-terminal SH3 domain of Grb2 showed that this domain
132   interacts with Btk, as well as with the ubiquitin ligase Cbl and SOS (Engels et al., 2014).
133   Substitution of the N-terminal SH3 domain of Grb2 by the C-terminal SH3 domain of Grb2, or

134   by the N-terminal SH3 domain of the Grb2 family member GRAP resulted in failure to trigger
135   Ca^{2+} flux. In the mIgG fusion with the N-terminal SH3 domain of GRAP, Ca^{2+} flux was restored
136   by the substitution of three residues in the GRAP SH3 domain by the corresponding residues in
137   Grb2 (Engels et al., 2014). Thus, an interaction between Grb2 and Btk plays a critical role in
138   BCR signaling.
139   We now report the discovery, made using *in-vitro* reconstitution of Btk on PIP_3-
140   containing membranes, that Btk and Grb2 interact through the proline-rich linker of Btk, and
141   that, through this interaction, Grb2 strongly stimulates the kinase activity of Btk. Our data
142   indicate that membrane recruitment of Btk by PIP_3 is insufficient for potent activation of Btk,
143   which requires interaction with Grb2 at the membrane. The activation of Btk by Grb2 relies
144   primarily on the N-terminal SH3 domain of Grb2 and does not require that the SH2 domain be
145   able to bind to phosphotyrosine residues – we infer that the SH2 domain is free to interact with
146   phosphotyrosine residues presented by scaffold proteins. Our data suggest a potential mechanism
147   whereby the binding of one SH3 domain of Grb2 to the proline-rich linker of Btk enables the
148   other SH3 domain to bind to the SH2-kinase linker of Btk, thereby displacing the inhibitory
149   intramolecular interaction of the Btk SH3 domain. Thus, the interaction between Grb2 and Btk
150   can integrate the localization of Btk with its activation.
151
152   **Results and Discussion**
153
154   *Btk recruits Grb2 to PIP_3-containing supported-lipid bilayers through the proline-rich region of*
155   *Btk*
156   To probe the interaction between Btk and Grb2, we utilized a supported-lipid bilayer
157   system that we had used previously to characterize the interaction of the isolated Btk PH-TH
158   module with lipids (Chung et al., 2019). Using this system we discovered, unexpectedly, that
159   Grb2 can be recruited to the membrane via an interaction with membrane-bound full-length Btk.
160   We had shown previously that the PH-TH module of Btk is recruited to membranes containing
161   4% PIP_3, and that this recruitment exhibits a sharp dependence on PIP_3 concentration in the
162   membrane. To characterize the interaction between Grb2 and full-length Btk we used supported-
163   lipid bilayers containing 4% PIP_3, to which full-length Btk is recruited from solution via the PH-
164   TH module (Chung et al., 2019). We found that recruitment of Btk to the membrane also
165   resulted in Grb2 being recruited to the membrane.
166   Recruitment of Grb2 to the membrane was measured using total internal reflection
167   fluorescence (TIRF) microscopy and Grb2 labeled with Alexa Fluor 647 (Grb2-647). The
168   surface sensitivity of TIRF imaging provides a highly selective measurement of membrane-
169   associated Grb2-647, without picking up signal from protein in the solution phase (Huang,
170   Ditlev, Chiang, Rosen, & Groves, 2017). When Btk and Grb2-647 were added together, Grb2-
171   647 was recruited to the bilayer, as indicated by an increase in fluorescence (Figure 2A). When
172   Grb2-647 was added to the supported-lipid bilayers without Btk there was no change in
173   fluorescence above background (Figure 2A). These experiments indicate that Grb2 is capable of
174   binding directly to Btk in the absence of other proteins. We confirmed that the observed
175   fluorescence change was not due to an irreversible process, such as protein aggregation, by
176   showing that the increase in fluorescence could be reversed rapidly by addition of unlabeled
177   Grb2 at a five-fold higher solution concentration than labeled Grb2 (Figure 2B).
178   We next addressed the question of which regions of Btk are necessary for the interaction
179   with Grb2. To do this, we tethered various constructs of Btk to membranes containing DGS-

5

180   NTA(Ni) (1,2-dioleoyl-sn-glycero-3-[(N-(5-amino-1-carboxypentyl)iminodiacetic acid)succinyl]
181   (nickel salt)) lipids by using an N-terminal hexa-histidine tag on Btk, rather than relying on the
182   binding of the PH-TH module to PIP$_3$. Constructs of N-terminally His-tagged Btk could then be
183   tethered directly to the membrane through the binding of the histidine tag to DGS-NTA(Ni)
184   lipids. This tethering method has been shown to result in limited unbinding of the His-tagged
185   protein over the timescale of our experiments (less than one hour) (Nye & Groves, 2008). This
186   allowed us to study the binding of Grb2 to constructs of Btk that do not contain the PH-TH
187   module (see Materials and Methods for precise definition of the Btk and Grb2 constructs).
188   Supported-lipid bilayers containing 4% DGS-NTA(Ni) were prepared and His-tagged
189   Btk constructs were added to these bilayers at different concentrations. Each of the following
190   constructs was tested by adding Grb2-647 and monitoring the change in TIRF intensity at the
191   membrane: full-length Btk, Btk in which the PH-TH module and proline-rich linker are deleted
192   (SH3-SH2-kinase; residues 212-659 of human Btk), SH2-kinase (residues 281-659), the kinase
193   domain alone (residues 402-659), and the proline-rich linker alone (residues 171-214). Grb2-647
194   is recruited to the bilayer when full-length Btk or the isolated proline-rich linker are tethered to
195   the membrane. The tethering of other constructs to the membrane did not show an intensity
196   change above background upon addition of labeled Grb2 (Figure 2C).
197   The Btk constructs used in these experiments were expressed using a bacterial system in
198   which co-expression of a tyrosine phosphatase is expected to maintain the proteins in the
199   unphosphorylated state, despite the presence of the Btk kinase domain in some of the constructs
200   (Seeliger et al., 2005; Wang et al., 2015). We checked the phosphorylation state of full-length
201   Btk used in these experiments by Western blot analysis of the protein with a pan-
202   phosphotyrosine antibody, as well as by mass spectrometry, and observed that purified Btk was
203   not phosphorylated. The interaction of Btk with Grb2 is therefore not dependent on an SH2-
204   phosphotyrosine interaction.
205   These experiments demonstrate that the proline-rich linker of Btk is able to recruit Grb2
206   to the membrane, without the other domains of Btk being present. No binding is detected to
207   constructs which lack the PH-TH module and the proline-rich linker. The set of experiments with
208   His-tagged Btk also show that the interaction between Btk and Grb2 is not dependent on Btk
209   binding to PIP$_3$ in the membrane, since there is no PIP$_3$ present in these experiments. We
210   conclude that the proline-rich linker is a principal determinant of the interaction between Btk and
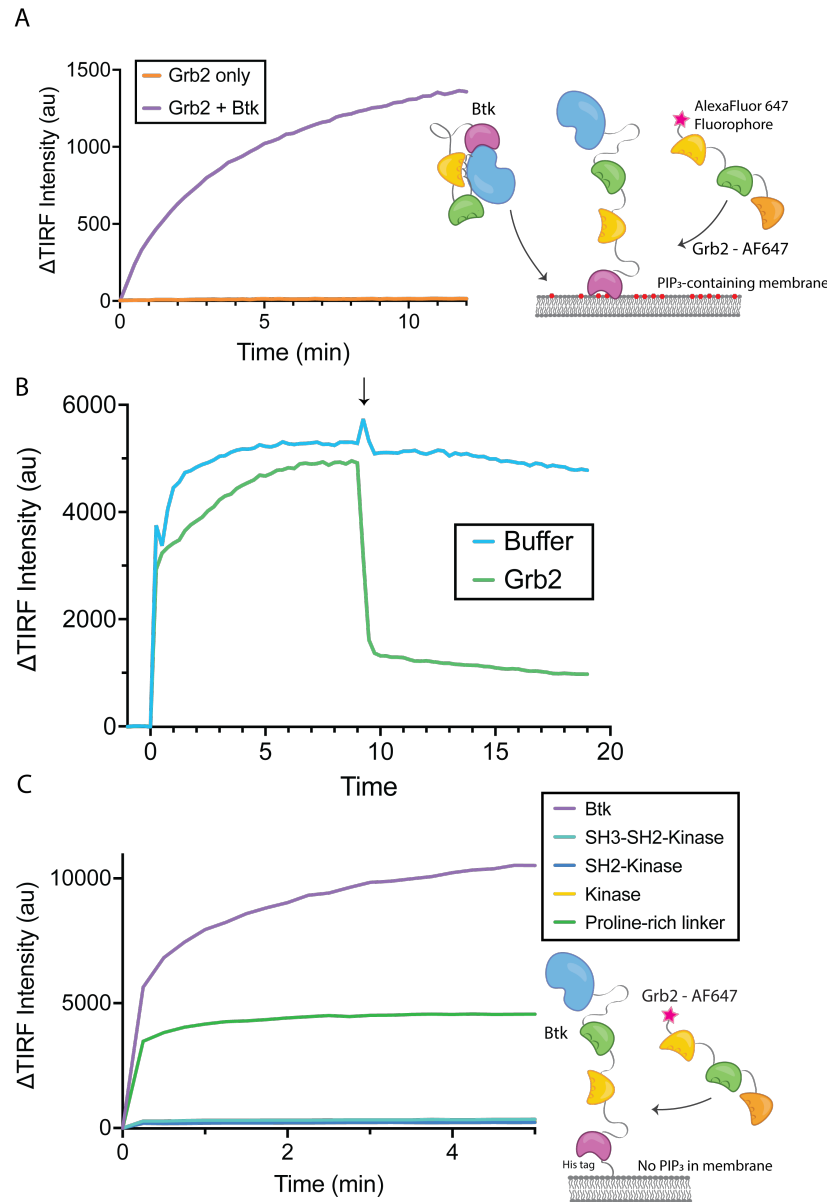211   Grb2.

212
213
214 **Figure 2. Grb2 interacts with membrane-bound Btk.** A) Fluorescently labeled Grb2 was
215 added to supported-lipid bilayers containing 4% PIP$_3$, with or without Btk. The change in
216 fluorescence intensity, monitored by TIRF, is plotted over time. B) The binding of Grb2 to
217 membrane bound Btk is reversible. Grb2 was added to a bilayer decorated with His-tagged Btk.
218 In the blue curve, the bilayer is washed with buffer, the arrow indicates when the wash occurred.
219 In one experiment (blue graph), the bilayer was washed with buffer. In another experiment
220 (green graph), the bilayer was washed with a solution containing 10-fold higher concentration of
221 unlabeled Grb2. C) Various constructs of Btk (Btk, SH3-SH2-Kinase, SH2-Kinase, Proline-rich
222 linker) with His tags were tethered to supported-lipid bilayers containing 4% DGS-NTA(Ni)
223 lipids. The bilayers were washed after equilibration to remove any weakly bound Btk.
224 Fluorescently-labeled Grb2 was added to these bilayers and the change in fluorescence intensity
225 with time is shown. Each experiment shown here was carried out in at least triplicate, though
226 only one experiment is plotted for each as exact intensity varies with each bilayer preparation.

7

227

228

229   *Grb2 enhances the kinase activity of Btk*

230   Btk is activated by PIP_3-containing vesicles, as shown by experiments in which the

231   phosphorylation of full-length Btk was monitored by Western blot with pan-phosphotyrosine

232   antibody (Wang et al., 2015). We repeated those experiments by incubating Btk (1 µM bulk

233   solution concentration) in the presence or absence of lipid vesicles containing 4% PIP_3, and

234   added increasing concentrations of Grb2, from 0-10 µM bulk solution concentration. In the

235   absence of vesicles, no change in phosphorylation is detected when Grb2 is added to Btk (Figure

236   3A-B, and Figure 3 – supplement 1). In the presence of PIP_3-containing vesicles, the addition of

237   Grb2 results in substantially increased levels of Btk phosphorylation, compared to the presence

238   of PIP_3-containing vesicles alone. When Btk is mixed with Grb2, the phosphorylation level

239   detected at 5 minutes after initiation of the reaction is comparable to that seen at 20 minutes for

240   Btk without Grb2 (Figure 3A-B and Figure 3 – supplement 1). Initiation of the kinase reaction

241   also results in phosphorylation of Grb2 (Figure 3C and Figure 3 – supplement 2).

242   We tested whether the binding of Grb2 to Btk influences the ability of Btk to

243   phosphorylate its specific substrate, $PLC\gamma2$. To do this we monitored phosphorylation of a

244   peptide segment spanning residues 746 to 766 of $PLC\gamma2$ that contains two tyrosine residues.

245   Phosphorylation of this segment by Btk plays a key role in activation of $PLC\gamma2$ in B cells

246   (Ozdener, Dangelmaier, Ashby, Kunapuli, & Daniel, 2002; Rodriguez et al., 2001). This peptide

247   segment was fused to an N-terminal SUMO protein and a C-terminal Green fluorescent protein

248   (GFP) (referred to as the $PLC\gamma2$-peptide fusion) to allow for visualization on a gel, as the

249   substrate is otherwise too small to analyze by Western blot. We added Btk to PIP_3-containing

250   vesicles in the presence of $PLC\gamma2$-peptide fusion, with or without the addition of Grb2 (Wang et

251   al., 2015). Phosphorylation of $PLC\gamma2$-peptide fusion was measured by Western blot analysis of

252   total phosphotyrosine. Under these conditions, the presence of Grb2 enhances phosphorylation of

253   the $PLC\gamma2$-peptide fusion substantially (Figure 3C-D and Figure 3 – supplement 2). For

254   example, 20 minutes after initiation of the kinase reaction, the level of phosphorylation as

255   detected by Western blot is increased by about three times in the presence of Grb2.

256   Detectable activation of Btk by Grb2 only occurs when the PH-TH module of Btk

257   engages PIP_3 at the membrane. This is an important point, because Grb2 is a ubiquitous protein

258   that is involved in many different signaling pathways and is expressed constitutively (Hein et al.,

259   2015; Shi et al., 2016). Our results show that Grb2 activation of Btk is layered upon a necessary

260   first step of PIP_3 generation, which requires BCR stimulation. Enhanced activation of Btk results

261   in increased phosphorylation of Btk itself as well as phosphorylation of the $PLC\gamma2$-peptide
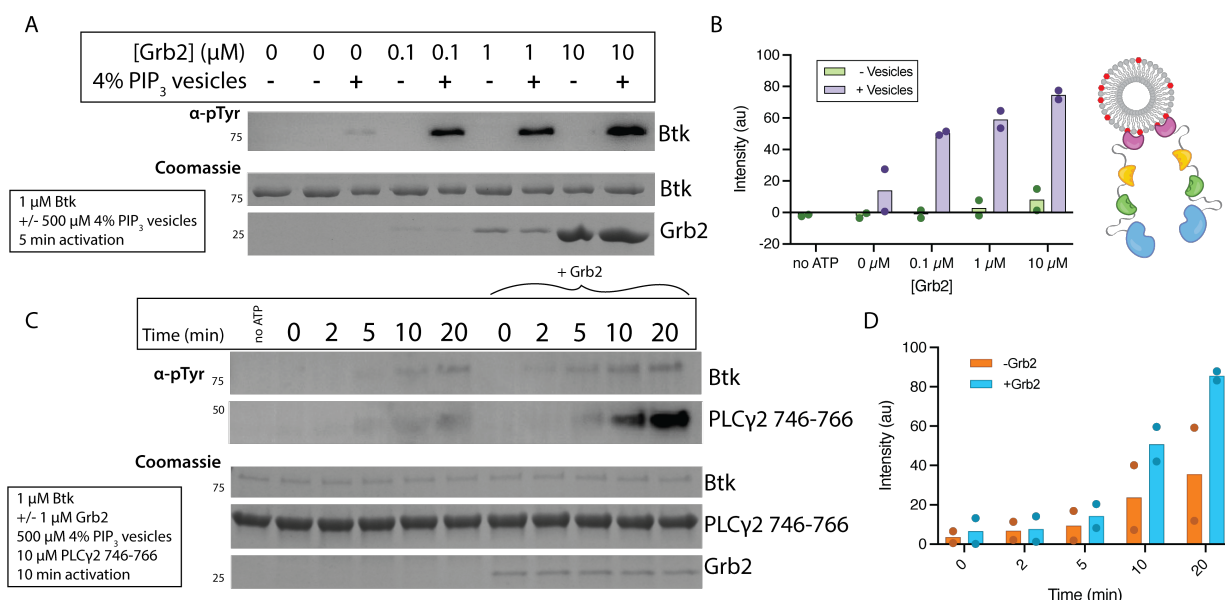
262   fusion.

263

Figure 3. Grb2 enhances Btk kinase activity in a PIP$_3$ dependent manner. The activity of Btk is monitored by measuring the phosphorylation of Btk, Grb2, and a PLCγ2-peptide fusion protein. A) Grb2 was titrated into samples containing Btk with or without 4% PIP$_3$ lipid vesicles. These samples were activated for 5 minutes and then quenched. Total phosphorylation was measured by Western blot. See Figure 3 Supplement 1 for independent experiment replicate. B) Quantification of Btk phosphorylation measured from (A) along with one independent experiment replicate, bar represents the mean intensity. C) All samples contain Btk, PLCγ2-peptide fusion and 4% PIP$_3$ lipid vesicles. Samples were activated and quenched at the timepoints listed (0-20 minutes), the left and right sides of the blot compare samples without or with Grb2. See Figure 3 Supplement 2 for independent experiment replicate. D) Quantification of PLCγ2-peptide fusion phosphorylation measured from (C), along with one independent experiment replicate, bar represents the mean intensity.
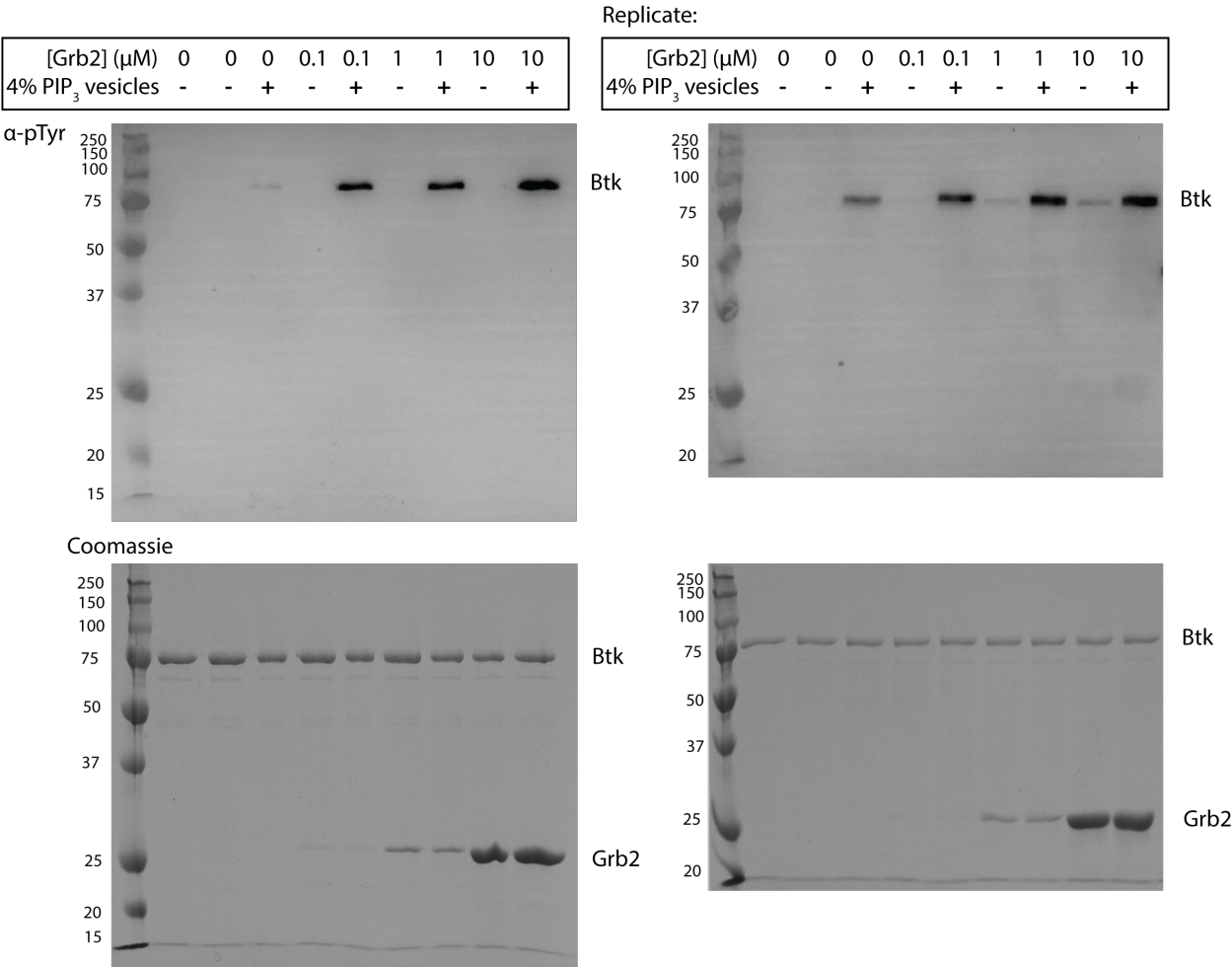
9

Figure 3 Supplement 1. Grb2 enhances *trans*-autophosphorylation of Btk in the presence of PIP₃ containing vesicles. Entire blot from Figure 3A in replicate, looking at autophosphorylation of Btk. For each lane 1 µM Btk was activated for 5 min in the presence or absence of 500 µM lipids, single unilamellar vesicles containing 4% PIP₃, and the indicated concentrations of Grb2. Each experiment was carried out in at least duplicate.
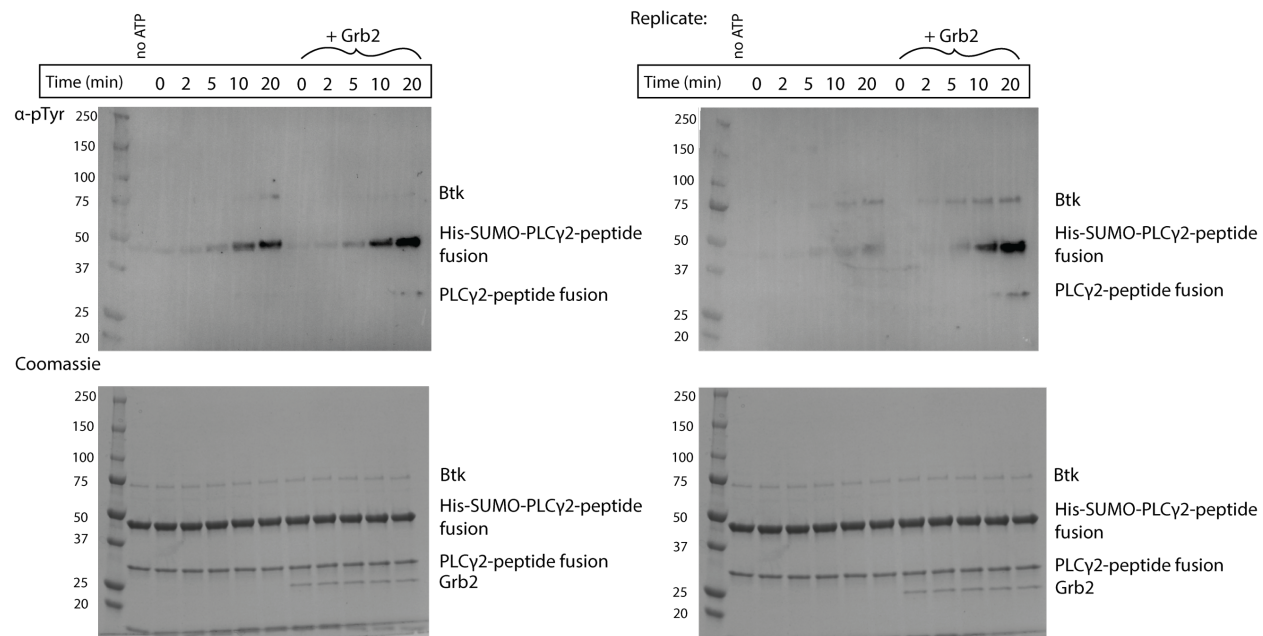
10

Figure 3 Supplement 2. Grb2 enhances phosphorylation of PLCγ2 by Btk in the presence of PIP₃ containing vesicles. Entire blot from Figure 3C in replicate, looking at phosphorylation of PLCγ2-peptide fusion. 1 µM Btk was activated for the indicated amount of time in the presence of 500 µM lipids, single unilamellar vesicles containing 4% PIP₃, 10 µM PLCγ2 peptide fusion with or without 1µM Grb2. Each experiment was carried out in at least duplicate.

All three domains of Grb2 are necessary for stimulation of Btk kinase activity

We made constructs corresponding to each individual domain of Grb2 (N-terminal SH3, SH2, and C-terminal SH3), or combinations of domains (N-terminal SH3-SH2, SH2-C-terminal SH3, and N-terminal SH3-C-terminal SH3, see Materials and Methods for the specification of these constructs). We made a Grb2 variant, R86K in which a conserved arginine residue in the SH2 domain that is critical for phosphotyrosine binding is mutated to lysine. Substitution of the corresponding arginine residue in other SH2 domains attenuates the binding of the SH2 domains to phosphorylated peptides (Mayer, Jackson, Van Etten, & Baltimore, 1992). We have demonstrated recently that the R86K mutation impairs the ability of Grb2 to promote phase separation of scaffold proteins (C.-W. Lin et al., 2022). Another Grb2 variant (Y160E) has a reduced capacity for dimerization (Ahmed et al., 2015). The ability of each of these constructs to stimulate Btk activity was tested, as measured by phosphorylation of the PLCγ2-peptide fusion (Figure 4A and Figure 4 – supplement 1). All reactions were carried out in the presence of unilamellar vesicles at a total lipid concentration of 500 µM containing 4% PIP₃. Protein and vesicles were incubated together for 15 minutes in the absence of ATP, and the reaction time is measured from when ATP was added to the solution.

Full-length Grb2 increases the phosphorylation of the PLCγ2-peptide fusion by six-fold relative to the reaction in which no Grb2 was added (Figure 4 and Figure 4 – supplement 1 and 2). The Grb2 variant in which the ability of the SH2 domain to bind to phosphopeptides is impaired (Grb2 R86K) stimulates the reaction to essentially the same extent as wild-type Grb2, indicating that the phosphopeptide-binding ability of the Grb2 SH2 domain is not required for

11

316   stimulation of Btk activity by Grb2. This observation suggests that Grb2 bound to Btk will retain
317   the capacity to dock on phosphorylated scaffold proteins via the SH2 domain, as discussed
318   below. Removal of any of the three component domains of Grb2 results in substantial reduction
319   of phosphorylation of the PLCγ2-peptide fusion (Figure 4 and Figure 4 – supplement 1 and 2).
320   The crystal structure of Grb2 (PDB code 1GRI) shows the formation of a Grb2 dimer in
321   which there are extensive interactions between the SH3 domains of one Grb2 molecule and the
322   SH2 domain of the other (Maignan et al., 1995). In our experiments, the stimulatory effects of
323   Grb2 on Btk activity are observed only when Btk is localized to the membrane, and is at high
324   local concentration, thus potentially promoting Grb2 dimerization. Deletion of the SH2 domain
325   would disrupt the dimeric arrangement seen in the crystal structure. Mutation of Tyr 160 in
326   Grb2, located at the distal surface of the SH2 domain and involved in the inter-subunit contacts
327   in the crystallographic dimer, has been shown previously to affect Grb2 dimerization (Ahmed et
328   al., 2015; C.-C. Lin et al., 2012). More recently, we have shown that the Y160E Grb2 mutant is
329   defective in promoting phase separation of scaffold proteins upon phosphorylation (C.-W. Lin et
330   al., 2021). In the present study, the use of Grb2-Y160E shows a reduction in the PLCγ2-peptide
331   fusion phosphorylation by Btk, compared to the wild-type Grb2. This result indicates that Grb2
332   dimerization may be important for stimulation of Btk activity, although a definitive analysis of
333   the mechanism awaits further study of additional Grb2 mutants.
334   Constructs containing only the N-terminal SH3 domain of Grb2 consistently have a larger
335   effect on phosphorylation than constructs containing only the C-terminal SH3 domain (Figure
336   4A-B and Figure 4 – supplement 1). This indicates that the N-terminal SH3 domain is more
337   important for the interaction with Grb2, consistent with the earlier finding that fusion of the N-
338   terminal SH3 domain of Grb2 to mIgG is sufficient for promoting Ca^{2+} flux through Btk (Engels
339   et al., 2014).
340   We studied a shorter Btk construct corresponding to the Src module (SH3-SH2-Kinase),
341   which lacks the PH-TH module and the PH-TH-SH3 linker. We monitored the phosphorylation
342   of this construct using the Western blot assay. This construct is much more active than the full-
343   length construct and its activity is not dependent on lipids, due to the lack of a PH-TH module
344   (Wang et al., 2015). Each reaction condition contained 1 μM Btk, 10 μM PLCγ2-peptide fusion
345   and either 0 or 10 μM Grb2. Reactions were quenched at a range of timepoints from 2 to 10
346   minutes, and phosphorylation levels on Btk and PLCγ2-peptide fusion were measured separately
347   (Fig 4C-D and Figure 4 – supplement 2). Phosphorylation on Btk increase slightly in the
348   presence of Grb2, while the levels of phosphorylation on the PLCγ2-peptide fusion are similar
349   with or without Grb2.
350   The slight stimulation by Grb2 of the autophosphorylation of the Src module construct of
351   Btk shows that Grb2 stimulation of Btk activity may also rely on elements additional to the
352   proline-rich linker and internal to the Src module. This points to the presence of another binding
353   site within Btk that is capable of interacting with Grb2. The Src-module construct of Btk
354   contains the SH2-kinase linker, which binds to the Btk SH3 domain in an intramolecular
355   interaction in the autoinhibited state (Moarefi et al., 1997; Moroco et al., 2014). One possible
356   explanation for the change in phosphorylation observed here is that Grb2 has some affinity for
357   the SH2-kinase linker and is able to release autoinhibition of the kinase by competing with the
358   Btk SH3 domain. We expect the intermolecular binding of an SH3 domain to the SH2-kinase
359   linker of Btk to be very weak, as demonstrated by the lack of Grb2 recruitment by this construct
360   when tethered to supported-lipid bilayers (Figure 2C). In the case of full-length Btk, this
361   competition could be assisted by one SH3 domain of Grb2 binding to the proline-rich linker and

362   promoting a pseudo-intramolecular binding of the second SH3 domain of Grb2 to the SH2-
363   kinase linker of Btk. These aspects of the interaction between Btk and Grb2 await future
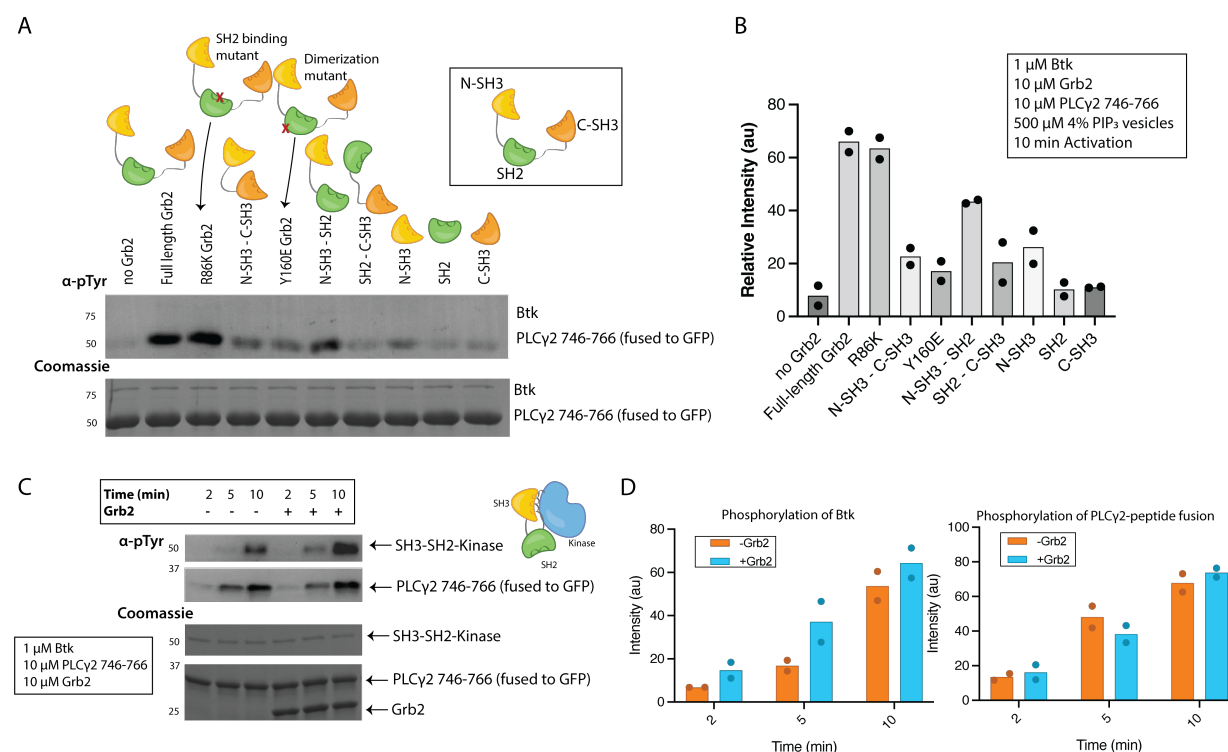364   experimentation for better understanding.
365

366
367   **Figure 4. Activation of full-length and truncated Btk by different Grb2 constructs.** A)
368   Phosphorylation of PLCγ2 peptide fusion by Btk in the presence of 4% PIP$_3$ lipid vesicles was
369   monitored in the presence of various Grb2 constructs. These constructs include: full length Grb2,
370   R86K, N-terminal SH3 fused to C-terminal SH3, Y160E, N-terminal SH3-SH2, SH2-C-terminal
371   SH3, N-terminal SH3, SH2, and C-terminal SH3. See Figure 4 Supplement 1 for independent
372   experiment replicate. B) Quantification of PLCγ2-peptide fusion phosphorylation measured from
373   (A), along with one independent experiment replicate, bar represents the mean intensity. C)
374   Activation of a truncated construct of Btk, SH3-SH2-kinase. Total phosphorylation was
375   monitored in the absence or presence of Grb2 over time. See Figure 4 Supplement 2 for
376   independent experiment replicate. D) Quantification of Btk phosphorylation or PLCγ2-peptide
377   fusion phosphorylation measured from (C), along with one independent experiment replicate, bar
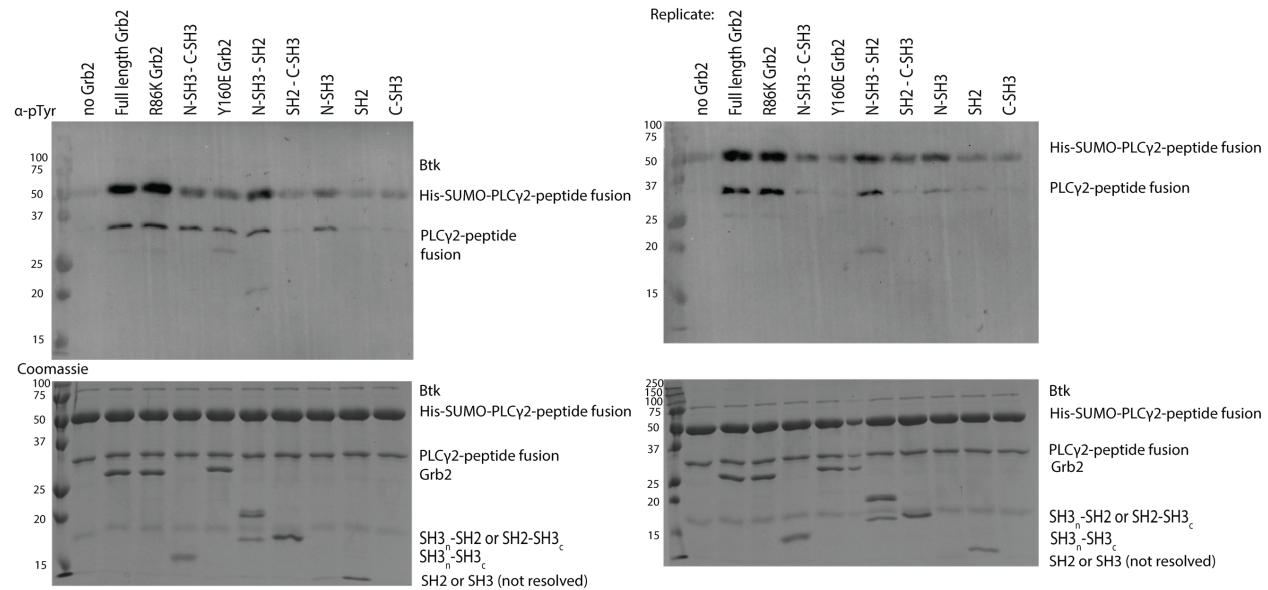378   represents the mean intensity.
379

13

Figure 4 Supplement 1. Phosphorylation of PLCγ2 by Btk with the addition of various Grb2 constructs. Entire blot from Figure 4A and replicate, looking at phosphorylation of PLCγ2-peptide fusion in the presence of Btk and varying constructs of Grb2. 1 µM Btk was activated for 10 minutes in the presence of 500 µM lipids, single unilamellar vesicles containing 4% PIP$_3$, 10 µM PLCγ2 peptide fusion with 10 µM of the indicated construct of Grb2. Each experiment was carried out in at least duplicate.
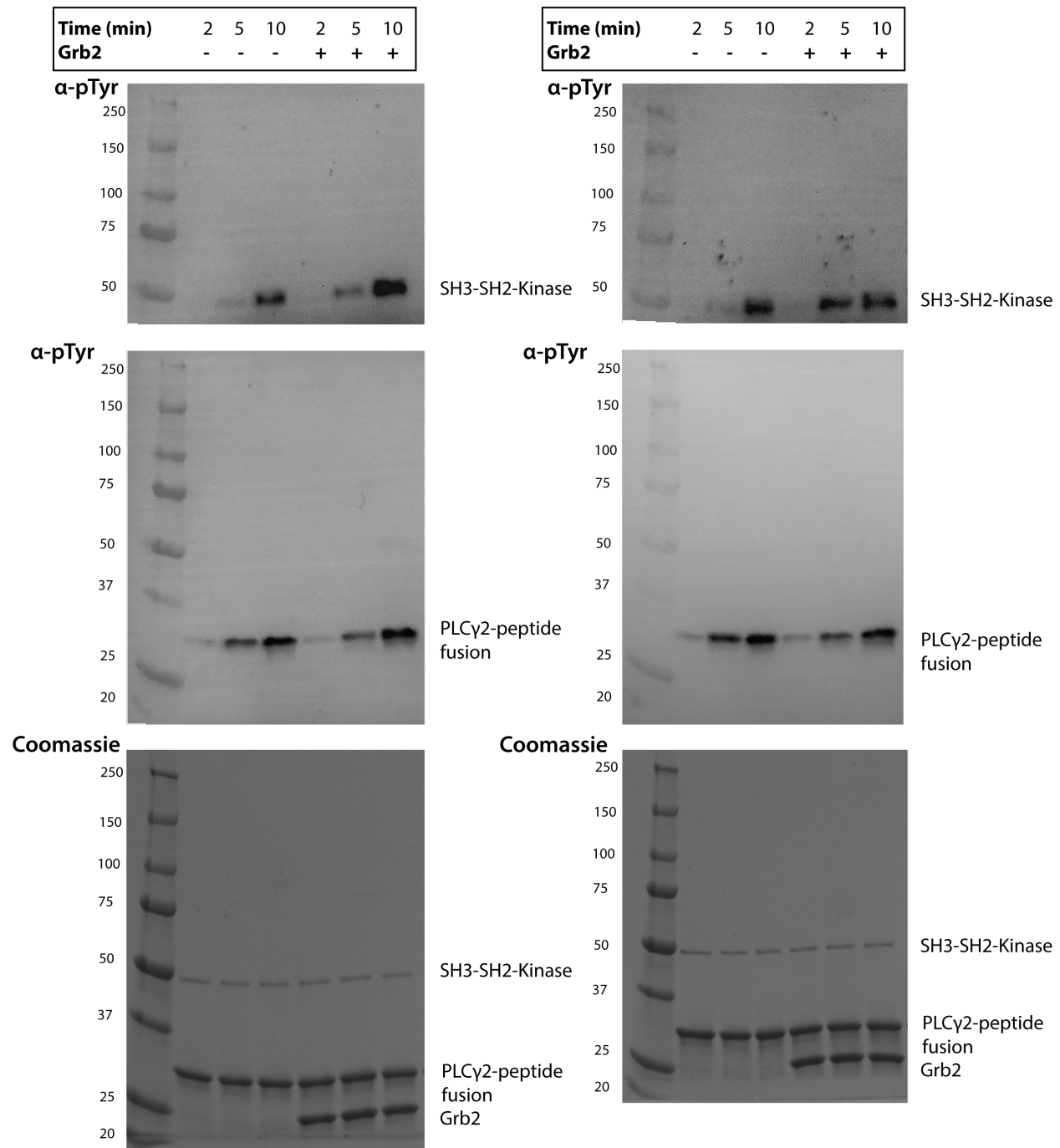
14

Figure 4 Supplement 2. The Src module of Btk shows moderate enhancement of catalytic activity upon addition of Grb2. Entire blot from Figure 4C and replicate, looking at phosphorylation of the Src-module of Btk with Grb2 and PLCγ2-peptide fusion. 1 µM Src-module of Btk was activated for the indicated amount of time in the presence of 10 µM PLCγ2 peptide fusion with 10 µM of Grb2. Each experiment was carried out in at least duplicate.

15

398   *Grb2 does not affect dimerization of Btk on the membrane and cannot rescue the catalytic*
399   *activity of a dimerization-deficient mutant of Btk*
400   Btk activation relies on homodimerization of the PH-TH modules (Chung et al., 2019;
401   Wang et al., 2015). Given this, it is possible that the two SH3 domains of Grb2 could promote
402   activation by facilitating dimerization by crosslinking two different Btk molecules. To check
403   whether Grb2 impacts the dimerization of Btk we measured the diffusion constant and the dwell
404   time of Btk on the membrane in the presence or absence of Grb2 (Figure 5A and Figure 5 –
405   supplement 1) (Chung et al., 2019). Although there is no simple relation connecting two-
406   dimensional diffusion and molecular complex size as there is for three-dimensional diffusion,
407   two-dimensional diffusion on a membrane surface nonetheless changes markedly between
408   monomers and dimers and is a sensitive measurement of dimerization (Chung et al., 2018, 2019;
409   Kaizuka & Groves, 2004; Knight & Falke, 2009). If Grb2 increases the population of Btk
410   dimers, we would expect to see a decrease in the diffusion constant of individual complexes on
411   the membrane in the presence of Grb2. If Grb2 increases the affinity of Btk for the membrane,
412   this would be manifested as an increase in Btk dwell time, the time that single molecules of Btk
413   stay at the membrane, through a reduction in off-rate.
414   To enable site-specific labeling of full-length Btk we used unnatural amino acid
415   incorporation of an azido-phenylalanine (AzF) group on the surface of the kinase domain of Btk
416   (Chatterjee, Sun, Furman, Xiao, & Schultz, 2013; Chin et al., 2002). AzF enables the use of an
417   azide-reactive dye to label the protein and eliminates non-specific labeling at other sites (see
418   Materials and Methods for details). Several sites were tested, and incorporation of AzF at
419   position 403 (Thr 403 in wild-type Btk) showed the best yield of labeled Btk. Thr 403 is a
420   surface-exposed sidechain in the N-lobe of the kinase domain , and we do not anticipate that
421   incorporation of AzF at this position will disturb the structure of Btk. For all data utilizing
422   fluorescent full-length Btk, the construct used is Btk T403AzF labeled with azide reactive Cy5
423   (Btk-Cy5).
424   The surface density of Btk-Cy5 on the membrane was observed to increase when the
425   solution concentration of unlabeled Btk was increased from 0 nM to 20 nM, in the presence of
426   very low concentrations of Btk-Cy5 (500 pM-1 nM). This enables the monitoring of single
427   molecules of Btk-Cy5, which was done either in the presence of Grb2 at 50 nM bulk
428   concentration, or without Grb2. From each sample, step-size distributions were compiled from
429   the single-molecule trajectories to assess the various time-dependent components to Btk
430   diffusion on the membrane. Step-size distributions generally required fitting to three
431   components, while two-component exponential fits were sufficient for the binding dwell time
432   data. Both with and without Grb2, the fastest of the three diffusion constants (corresponding to
433   monomeric Btk) decreases with increasing Btk concentration, indicating the formation of Btk
434   dimers. The presence of Grb2 does not change the diffusive behavior of Btk at any of the
435   concentrations used in these experiments. The decrease in Btk diffusion constant with increasing
436   solution concentration of Btk is consistent with what is observed for the Btk PH-TH module at
437   these concentrations, confirming that full-length Btk interacts with the membrane in the same
438   way as does the Btk PH-TH module (Figure 5A and Figure 5 – supplement 1) (Chung et al.,
439   2019). These experiments show that Grb2 does not change the dynamics of membrane-bound
440   Btk, either through changes in the dimer population or changes in the membrane affinity.
441   We checked to see if the activity of a Btk mutant, K49S/R52S, which is incapable of
442   significant dimerization on the membrane, could be rescued by the addition of Grb2. The
443   K49S/R52S mutations eliminate a PIP$_3$ binding site and prevent dimerization of the PH-TH

444 module (Chung et al., 2019). A Western blot analysis shows no change in phosphorylation of the
445 mutant Btk upon addition of Grb2, over a range of Grb2 concentrations (Figure 5B-C and Figure
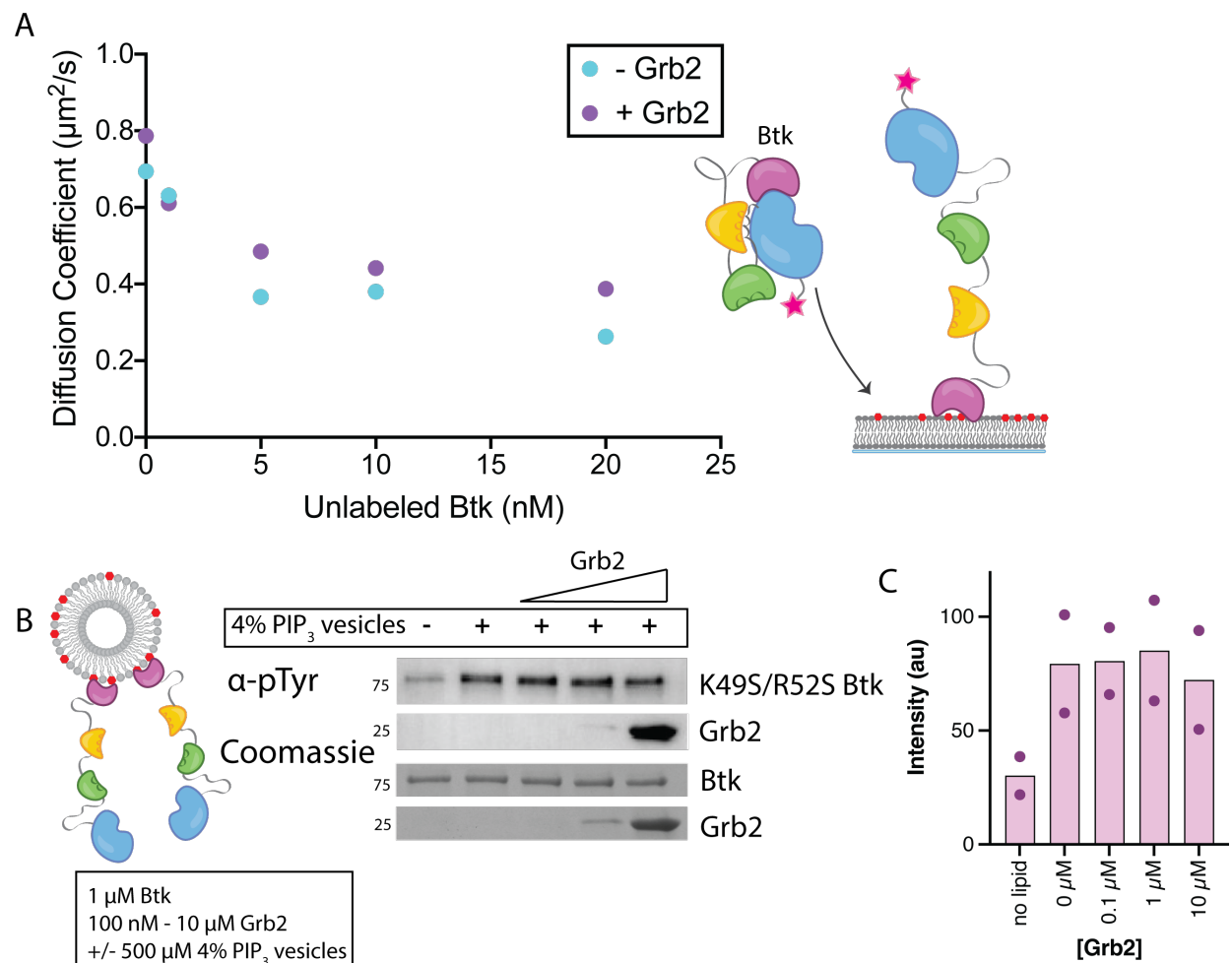446 5 – supplement 2).
447

448
449 **Figure 5. Grb2 does not enhance the dimerization of Btk on membranes.** A) Diffusion
450 constants for membrane bound Btk were determined by single-molecule tracking. Diffusion
451 constants are plotted as a function of solution concentration of unlabeled Btk for conditions with
452 or without Grb2. B) Western blot of Btk K49S/R52S (PH-TH peripheral PIP$_3$ binding site
453 mutant) phosphorylation with 4% PIP$_3$ while titrating the amount of Grb2. See Figure 5
454 Supplement 2 for independent experiment replicate. C) Quantification of Btk K49S/R52S
455 phosphorylation measured from (B), along with one independent experiment replicate, bar
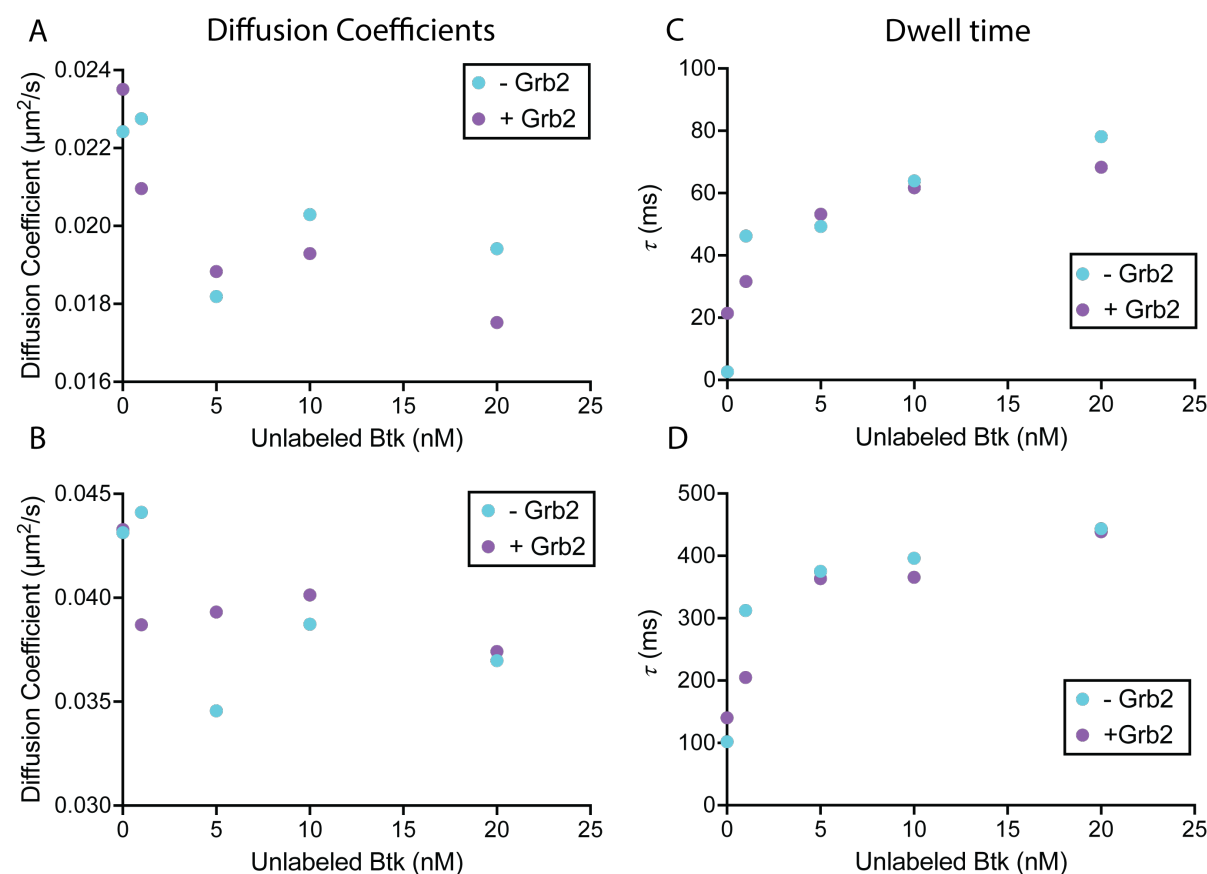456 represents the mean intensity.
457

17

458
459
460 **Figure 5 Supplement 1. The diffusion of Btk on membranes in the absence and presence of**
461 **Grb2.** Remaining components of Btk diffusion as fit by single molecule tracking. A) The
462 slowest component of the diffusion, trending slightly with increasing surface density of Btk. B)
463 The middle component of the diffusion, remaining relatively constant across Btk concentrations.
464 C) And D) are both components of the dwell time, which both show dependence on Btk surface
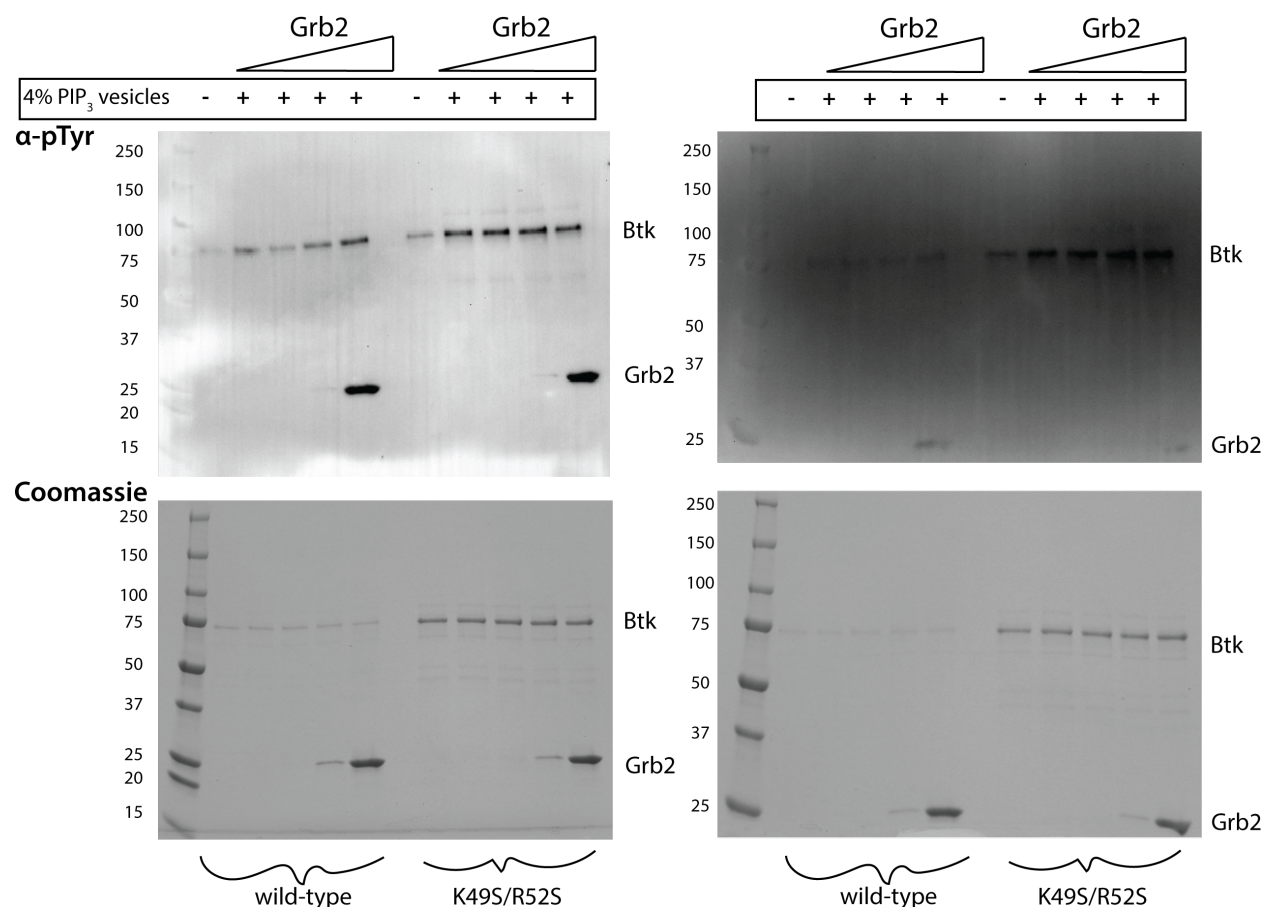465 density.
466

Figure 5 Supplement 2. Phosphorylation of Btk K49S/R52S is not enhanced by Grb2. Entire blot from Figure 5B and replicate looking at phosphorylation of Btk K49S/R52S with the addition of Grb2. 1 µM Btk wild-type or K49S/R52S was activated for 10 minutes in the presence or absence of 500 µM lipids, single unilamellar vesicles containing 4% PIP$_3$, and 100 nM - 10 µM of Grb2, each consecutive lane representing an increase in the Grb2 concentration by one order of magnitude. Each experiment was carried out in at least duplicate.

Grb2 can recruit Btk to clusters of scaffold proteins

We studied how the ability of Grb2 to bind to Btk might impact the localization of Btk on the membrane, by monitoring the interaction of Btk with the scaffold protein LAT on supported-lipid bilayers. LAT is similar to the B cell scaffolding protein SLP65/BLNK. Our use of LAT, rather than SLP65/BLNK, was predicated by our extensive prior work with LAT on supported-lipid bilayers (Hashimoto et al., 1999; Huang et al., 2019, 2016; Huang, Chiang, et al., 2017; Huang, Ditlev, et al., 2017; Koretzky et al., 2006; Su et al., 2016).

LAT signaling clusters can be generated from minimal components on supported-lipid bilayers. Bilayers containing 4% DGS-NTA(Ni) were prepared with both LAT and the Src-family kinase Hck tethered to the membrane through His-tags. LAT was phosphorylated by Hck, as described previously, before other components were added (Figure 6A) (Huang et al., 2019, 2016; Huang, Ditlev, et al., 2017). The diffusion constants for phosphorylated LAT and Hck are similar to those for the lipids under these conditions, indicating lack of clustering. Upon the

19

490   addition of Grb2 and the proline-rich region of the Ras activator SOS (SOS-PRR), the
491   phosphorylated LAT undergoes a protein condensation phase transition and forms gel-like
492   domains of protein-rich areas in which the LAT no longer diffuses freely (Figure 6B) (Huang,
493   Ditlev, et al., 2017; Su et al., 2016). This phase transition is thought to be analogous to the
494   formation of LAT signaling clusters in T cells (Ganti et al., 2020). Using this system, we
495   checked whether Btk could be recruited into the reconstituted LAT clusters through its
496   interaction with Grb2.
497   Btk was reconstituted on supported-lipid bilayers containing 4% PIP_3 and DGS-NTA(Ni)
498   lipids. LAT and Hck were tethered to these bilayers as well, as described above, and LAT was
499   phosphorylated by Hck. Subsequently, the components of the LAT signaling cluster were added
500   sequentially along with Btk. In one condition, Btk-Cy5 was added alone to the phosphorylated
501   LAT containing bilayers, in another condition Grb2 and Btk-Cy5 were added together, and a
502   third condition involved by Grb2, SOS-PRR and Btk-Cy5 (Figure 6A). For the final condition,
503   the bilayers were allowed to incubate for 1 hour to promote formation of the condensed-phase
504   LAT domains (Figure 6B). Fluorescently labeled SOS-PRR cannot be recruited to supported-
505   lipid bilayers containing Btk alone (Figure 6 – supplement 1).
506   Single molecules of Btk-Cy5 were tracked at several different positions on the bilayer for
507   each condition. These tracks were then used to compile a step-size distribution based on all Btk-
508   Cy5 tracks for a given condition, as described (J. J. Lin et al., 2020). The step-size distributions
509   reflect the diffusive behavior of the entire population of Btk under a given condition; the shorter
510   the step-sizes, the slower moving the Btk molecules. When Btk was incubated with
511   phosphorylated LAT alone the step-size distribution is similar to that obtained for low
512   concentrations of Btk alone on 4% PIP_3-containing supported-lipid bilayers (Figure 6C).
513   Addition of Grb2 shifts the step-size distribution to shorter steps, suggesting two possible
514   situations. One possibility is that, Grb2 is able to simultaneously bind Btk and LAT, thus slowing
515   Btk molecules through an additional anchor point to the membrane (via the Grb2-LAT complex).
516   The second possibility is that Grb2 alone promotes condensation of LAT (C.-W. Lin et al.,
517   2021), creating small domains of dense LAT, within which Btk cannot diffuse freely. The
518   addition of SOS-PRR along with Grb2 induces the full phase transition of the phosphorylated
519   LAT. The step-size distribution shifts even further left under this condition, suggesting that Btk
520   has been trapped within the LAT dense phase (Figure 6C). This observation suggests that Btk is
521   likely to be tethered to the phosphorylated LAT molecules through binding of the SH2 domain of
522   Grb2 to phosphotyrosine residues on LAT and binding of the SH3 domains of Grb2 to Btk. This
523   interaction leads to recruitment of Btk into the LAT condensate.
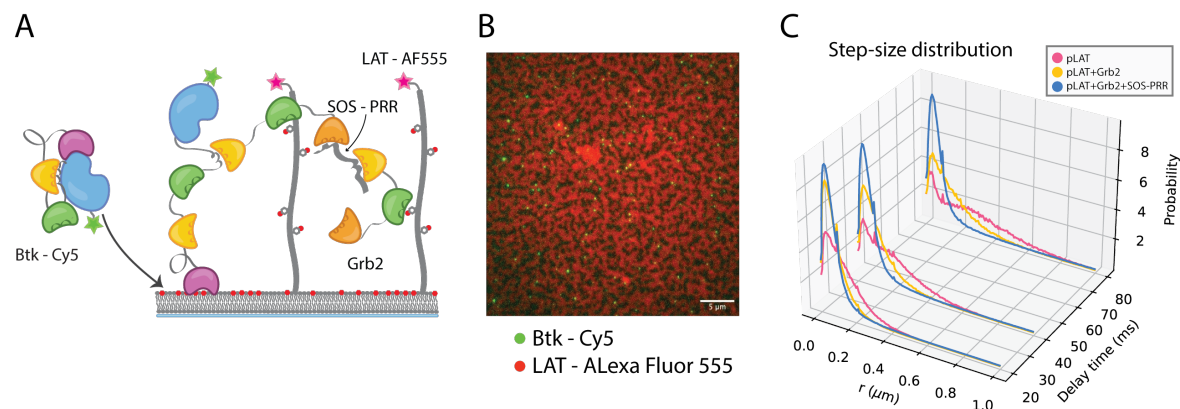524

Figure 6. Btk can be recruited to scaffold proteins through interaction with Grb2. A) Cartoon schematic of predicted mechanism for Btk recruitment into LAT signaling clusters. B) Overlay of image of Btk-Cy5 (green) and LAT-Alexa Fluor 555 (red) after LAT phase transition. C) Step-size distribution for Btk-Cy5 under each condition: phospho-LAT, phospho-LAT + Grb2, phase transitioned LAT (phospho-LAT + Grb2 + SOS-PRR). The step-size distribution was calculated at multiple delay times. Six different positions across the bilayer were analyzed of 500-600 frames, and one independent experiment was used to confirm trends observed here.
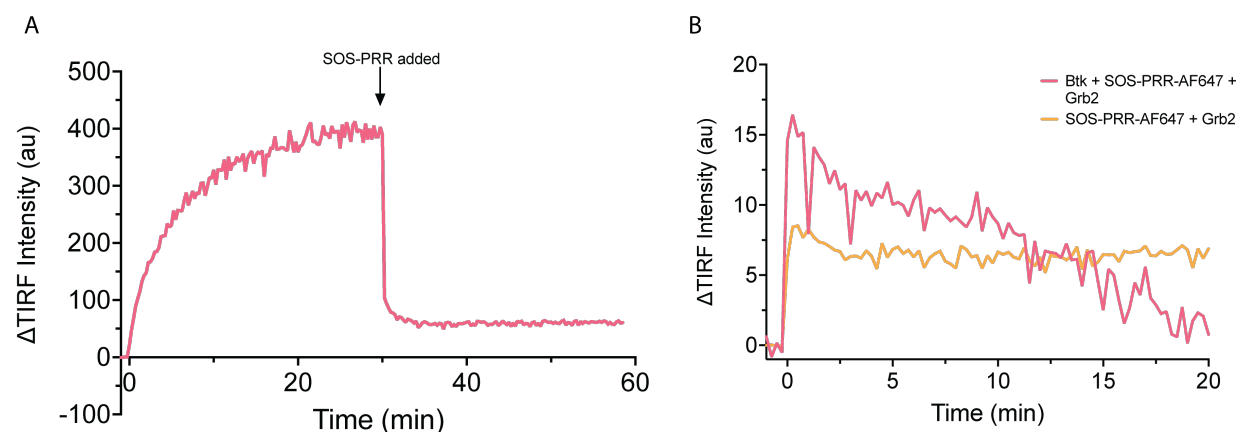

Figure 6 Supplement 1. Behavior of Btk on PIP3-containing membranes with the addition of SOS proline rich region. A) Here Grb2-AlexaFluor647 and Btk have been added to a PIP$_3$-containing membrane at time 0, AlexaFluor647 fluorescence intensity is measured. After 30 minutes SOS-PRR is added at the same concentration that is used in Figure 6. SOS-PRR appears to compete with Btk for Grb2 binding. B) Btk, Grb2, and SOS-PRR-AlexaFluor647 or Grb2 and SOS-PRR-AlexaFluor647 are added to PIP$_3$ containing membrane and AlexaFluor647 fluorescence intensity is measured. SOS-PRR does not interact with Btk on supported-lipid bilayers.

Ideas and speculation

The Tec kinases, including Btk and Itk, constitute one of three families of cytoplasmic tyrosine kinases that contain a conserved SH3-SH2-kinase unit known as the Src module (Shah

21

549 et al., 2018; Yeung et al., 2021). The other two kinase families that contain a Src module are the
550 Src-family kinases and the Abl family. The essential regulatory mechanism operative in these
551 kinases is an interaction between the SH3 domain and the linker connecting the SH2 domain to
552 the kinase domain – this interaction stabilizes the kinase domain in an autoinhibited
553 conformation, and displacement of the SH3 domain activates these kinases very strongly
554 (Moarefi et al., 1997).
555   The three Src-module families differ in terms of how additional elements in the kinase
556 support the autoinhibitory interaction between the SH3 domain and the SH2-kinase linker. The
557 kinase activity of the Src-family kinases is suppressed by phosphorylation of the C-terminal tail,
558 which organizes the SH3-SH2 unit into the inhibitory conformation. Abl is regulated by an N-
559 terminal capping segment that presents a myristoyl group that helps anchor the SH2 domain to
560 the kinase domain (Hantschel et al., 2003; Nagar et al., 2003).The N-terminal PH-TH module
561 shared by all Tec-family kinases is a critical and distinguishing element (Andreotti, Joseph,
562 Conley, Iwasa, & Berg, 2018; Devkota, Joseph, Boyken, Fulton, & Andreotti, 2017; Joseph et
563 al., 2017; Wang et al., 2015). In Btk, dimerization of the PH-TH module on membranes is
564 essential for activation, and this dimerization is promoted by the binding of the PH-TH module
565 to PIP_3 in the membrane (Chung et al., 2019; Wang et al., 2019, 2015). This mechanism is not a
566 universal feature of Tec kinase regulation – the PH-TH module of Itk, for example, does not
567 undergo dimerization on the membrane (Chung et al., 2019).
568   In this paper we present the discovery of an unexpected role for Grb2 in the control of
569 Btk activity. We show that Grb2 can bind and enhance the kinase activity of Btk in the presence
570 of PIP_3. Previous studies have shown that the Grb2 N-terminal SH3 domain could bind Btk
571 through interaction with the mIgG tails and SLP65 and potentiate downstream signaling (Engels
572 et al., 2014; Kurosaki & Tsukada, 2000). We propose that Grb2 binding could activate Btk by
573 displacing the Btk SH3 domain and releasing the inhibitory contacts within the Src module of
574 Btk (Figure 7). Elucidating the details of the activation mechanism requires further study. We
575 demonstrate that Btk kinase activity increases with the addition of Grb2 only with simultaneous
576 availability of PIP_3, which is an important point because Grb2 is a ubiquitous protein that is
577 highly expressed in many cell lines (Shi et al., 2016). This ensures that the Btk signal remains
578 responsive to activation of the B cell receptor.
579   A corollary of our findings is that membrane localization of Btk is insufficient for
580 maximal stimulation of Btk activity – the interaction of Btk with Grb2 at the membrane causes
581 increased Btk activity and stronger phosphorylation of PLCγ2. This fact may help reconcile
582 discrepancies between NMR studies of Btk autoinhibition (Joseph et al., 2017) and inferences
583 drawn from a crystal structure of a PH-TH-kinase construct of Btk (Wang et al., 2015). In the
584 crystal structure, the PH-TH module is docked on the C-helix in the N-lobe of the kinase domain,
585 and appears to stabilize an inactive conformation of the kinase domain. NMR analysis of Btk in
586 solution shows, however, that the interaction between the PH-TH module and the kinase domain
587 involves the activation loop, not helix C. An important point is that the crystal lattice is actually
588 formed by dimers of Btk, with the PH-TH module forming the canonical Saraste dimer while
589 docked on the C-helix of the inactive kinase domain (PDB 4Y93) (Wang et al., 2015). Thus the
590 crystal structure might represent a dimeric and autoinhibited form of Btk at the membrane, with
591 the PH-TH module forming the Saraste dimer. Grb2 might then serve to detach the PH-TH
592 module from the kinase domain, by binding the proline-rich linker (Figure 7). Testing such a
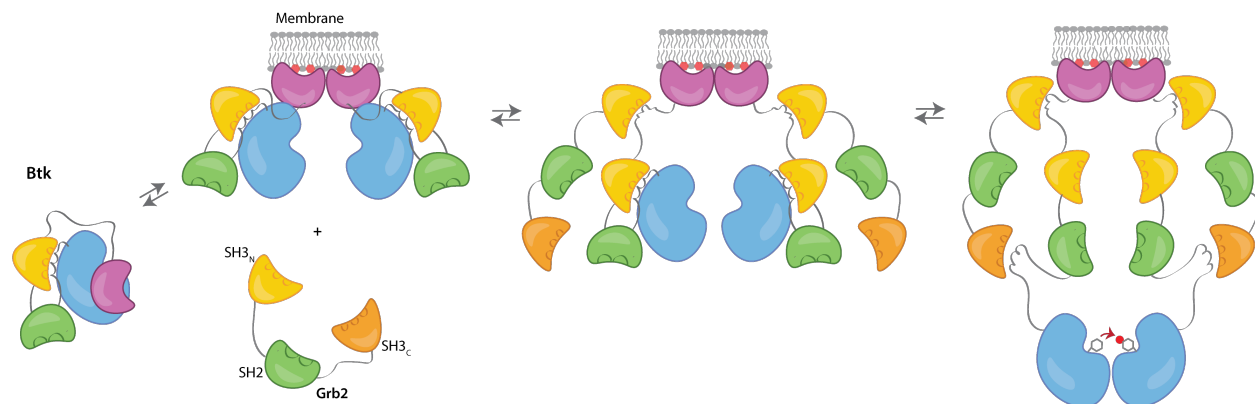593 model is an important direction for future work.
594

Figure 7. Grb2 enhances Btk activation at the membrane. Our data are consistent with a model in which PIP$_3$ binding at the membrane is not sufficient for full activation, and in fact Btk is still able to maintain some autoinhibition after membrane recruitment. Upon recruitment of Grb2 to the proline-rich linker of Btk, the second Grb2 SH3 domain is able to bind the SH2-kinase linker of Btk and displace Btk's SH3 domain, resulting in full release of autoinhibition.

By looking directly at Btk phosphorylation in the presence of Grb2 in our reconstituted system, we reveal an additional consequence of Grb2 binding – Grb2 binding can recruit Btk to signaling clusters at the membrane. In particular, the increased phosphorylation by Btk that we observe for a segment of PLCγ2 in the presence of Grb2 shows how Grb2 binding of Btk could have direct impact on the downstream signaling of Btk, subsequently increasing the population of active PLCγ2 molecules at the membrane. This is in line with observations in cells (Chiu, Dalton, Ishiai, Kurosaki, & Chan, 2002; Engels et al., 2014; Hashimoto et al., 1999; Kurosaki & Tsukada, 2000). In the absence of Grb2, Btk activation is slow, even when PIP$_3$ levels are high and can promote dimerization. In the presence of Grb2, Btk phosphorylation proceeds much more rapidly. This work illuminates a new level of regulation within Btk, in which optimal signaling may rely on interaction from an adaptor molecule that both stimulates activity and facilitates localization of Btk with downstream substrates.

23

615 **Materials and Methods**

616

617 *Construct definitions*

Construct	Gene	Vector	N-terminal Tag
Grb2	Full-length, UniProt P62993	pET28	His_6-TEV (Tobacco etch virus) site
Btk	Full-length, UniProt Q06187	pET28	His_6-SUMO
Btk SH3-SH2-kinase	Residues 212-659	pET28	His_6-SUMO
Btk SH2-Kinase	Residues 281-659	pET28	His_6-SUMO
Btk kinase	Residues 402-659	pET28	His_6-SUMO
Btk proline-rich linker	Residues 171-214	pET28	His_6-SUMO
PLCγ2-peptide fusion	PLCγ2 Residues 746-766 UniProt P16885, EGFP	pET28	His_6-SUMO
Grb2 SH3$_N$-SH2	Residues 1-153	pET28	His_6-TEV site
Grb2 SH2-SH3$_C$	Residues 60-217	pET28	His_6-TEV site
Grb2 SH3$_N$-SH3$_C$	Residues 1-59, 154-217	pET28	His_6-TEV site
Grb2 SH3$_N$	Residues 1-59	pET28	His_6-TEV site
Grb2 SH2	Residues 60-153	pET28	His_6-TEV site
Grb2 SH3$_C$	Residues 154-217	pET28	His_6-TEV site
Grb2 R86K	Full-length, R86K	pET28	His_6-TEV site
Grb2 Y160E	Full-length, Y160E	pET28	His_6-TEV site
Btk T403AzF	Full-length, T403Amber STOP	pET28	His_6-SUMO
Btk K49S/R52S	Full-length, K49S/R52S	pET28	His_6-SUMO
LAT	Residues 30-233, Uniprot O43561	pET28	His_6-TEV site
Hck	Residues 252-520, UniProt P08631	pET28	His_6-TEV site
SOS-PRR	Residues 1,051-1,333, UniProt Q07889	pET28	His_6-TEV site
YopH	UniProt P15273	pCDFDuet	

618

24

Protein preparation

For preparation of full-length Btk, the plasmid was transformed into BL21(DE3) *Escherichia coli* (*E. coli*) containing the YopH expression plasmid (described above) and plated on kanamycin and streptomycin containing agar plates (Seeliger et al., 2005). Transformed cells were first grown in a 200 mL Terrific broth containing 100 µg/mL kanamycin and streptomycin overnight culture at 37°C. This was then split into 6 L of Terrific broth containing 100 µg/mL kanamycin and streptomycin and grown to an optical density of 1-1.5 at 37°C. The cultures were mixed 1:1 with new media and antibiotic at 4°C and 1 mM isopropyl β-D-1-thiogalactopyranoside (IPTG) and maintained at 4°C to grow overnight. After overnight expression, the bacteria was spun down and resuspended in 15-30 mL of Ni A buffer (500 mM NaCl, 20 mM Tris-HCl pH 8.5, 20 mM Imidazole, 5% Glycerol). These were then flash frozen and kept at -80°C until the next step of the purification.

Cell pellets were thawed and then lysed by homogenization or sonication with addition of phenylmethylsulfonyl fluoride. The lysate was then spun down at 16500 rpm for one hour. Supernatant was collected and flowed over a HisTrap FF (GE) column. The column was then washed with 10 column volumes (CV) Ni A buffer, followed by four CV Ni B buffer (500 mM NaCl, 20 mM Tris-HCl pH 8.5, 500 mM Imidazole, 5% Glycerol). The elution fraction was then loaded onto a desalting column equilibrated in Buffer A (150 mM NaCl, 20 mM Tris-HCl pH 8.0, 5% Glycerol). The protein peak was collected and incubated with ULP1 protease overnight at 4°C.

After His tag cleavage, the sample was run over a second HisTrap column, this time the flow through and wash were collected. In some cases, a gradient of immidazole was applied as the Btk PH domain has some affinity for the Ni column even in the absence of the His tag. The protein was then concentrated in an Amicon Ultra centrifugal filter (Millipore Sigma) to less than 2 mL total volume. This was then loaded onto an S200 30/300 (GE) column equilibrated in Buffer A for biochemistry or Buffer B (150 mM NaCl, 50 mM Hepes pH 7.4, 5% Glycerol) for imaging studies. Fractions containing the purest target protein were collected and concentrated. These were then aliquoted and stored at -80°C after flash freezing.

All other constructs were purified in a similar manner with the following changes. All constructs that did not contain a kinase domain were transformed into BL21(DE3) *E. coli* without the YopH plasmid, and therefore they were grown with only kanamycin. Expression for these constructs was carried out overnight at 18°C. Grb2 constructs and PLCγ2-peptide fusion express at much higher levels than the Btk constructs and therefore only 1-2 liters were prepared at a given time, and therefore no overnight culture was required. For all constructs that contain a His tag after purification (LAT, Hck, and His-tagged Btk constructs), the protease and second HisTrap column were eliminated. Grb2 constructs and SOS-PRR each contain a TEV site and therefore TEV protease was used to remove the His tag.

Protein fluorescent labeling by maleimide conjugation

Grb2 and SOS-PRR were each prepared at a concentration of 50 µM and incubated with 5 mM DTT for 30 minutes on ice to ensure all accessible cysteines were reduced. Maleimide conjugated dye was dissolved in anhydrous DMSO and added in equimolar amounts to Grb2 or 3-fold molar excess to SOS-PRR and incubated at room temperature for 30 minutes or at 4°C overnight, depending on the stability of the protein. The reaction was then quenched with 10 mM DTT for 30 minutes at 4°C. After quenching, the protein was diluted in 10 – 15 mL fresh buffer, and then concentrated in an Amicon Ultra centrifugal filter, allowing free dye to be removed in

25

665 the flow through. This process was continued until no more free dye could be easily detected in
666 the flow through. At this point the protein was then purified by gel filtration in Buffer B as
667 described above. Labeling efficiency was calculated based on the absorbances at 280 nm and the
668 peak excitation wavelength for the dye, taking into account dye contribution to the 280 nm
669 signal. A note about Grb2 labeling: the protein tends to aggregate when exposed to an excess of
670 dye, and therefore we favored under labeling by only providing equimolar amount of dye.
671
672 *Protein fluorescent labeling by azido phenylalanine incorporation*
673 For site specific labeling of full-length Btk for single molecule studies, we used unnatural
674 amino acid incorporation of an Azido phenylalanine (AzF) residue (Amiram et al., 2015; Bard &
675 Martin, 2018; Chatterjee et al., 2013; Chin et al., 2002). An amber codon (UAG) was introduced
676 at the desired labeling position in the plasmid for Btk expression, and it was ensured that the stop
677 codon for this gene was not amber. This plasmid was co-transformed into BL21(DE3) containing
678 a plasmid expressing YopH with the pUltra-pAzFRS plasmid. A 5 mL starter culture was grown
679 overnight in TB at 37°C from this transformation. This was used to inoculate 1 L TB the
680 following morning which was grown to an optical density between 0.5 and 1 at 37°C. This
681 culture was spun down and resuspended in 167 mL cold (4°C) TB containing 2 mM AzF, before
682 induction, this culture was allowed to grow for 1.25 hours at 4°C. The culture was then induced
683 with 1 mM IPTG and grown overnight at 4°C. After this, protein purification proceeded as
684 normal until just before the gel filtration step, except that all reducing agents were left out of the
685 buffers. Yield of the protein is drastically reduced, however for our applications a low yield was
686 not a problem as long as labeling was feasible.
687 For labeling, the purified protein was concentrated to about 300 µL. 5 mM 5,5-dithio-bis-
688 (2-nitrobenzoic acid) (DTNB, Ellman's reagent) was prepared in 50 mM HEPES, pH 7.0, 250
689 mM KCl, 5% glycerol. DTNB was added at 15X molar excess to the protein solution and
690 incubated at room temperature for 10 minutes. The protein was then cooled back to 4°C and 300
691 µM dibenzocyclooctyl (DBCO)-Cy5 was added from a 30 mM stock in DMSO. This was
692 incubated overnight at 4°C. The reaction was quenched with 5 mM DTT and incubated at 4°C for
693 1 hour. At this point the labeled protein was purified by gel filtration, then concentrated to an
694 appropriate concentration, flash frozen and stored at -80°C. This protocol was adapted from the
695 lab of Andreas Martin (Bard, Bashore, Dong, & Martin, 2019; Bard & Martin, 2018; Lander et
696 al., 2012).
697

698 *Western blot assays for Btk kinase activity*
699 Samples were prepared with 2X concentration of each component depending on the
700 condition to be tested (2 µM Btk, 1 mM 4% PIP$_3$ single unilamellar vesicles (SUVs), 0-20 µM
701 Grb2) in Buffer A, final concentrations during the reaction are indicated for each blot (Figure
702 3A, 3C, 4A, 4C and 5B). These components were incubated for 15 minutes at room temperature
703 and then diluted 1:1 in activation buffer (20 mM MgCl$_2$, 2 mM ATP, 2 mM sodium vanadate).
704 These were mixed and the reaction proceeded at room temperature for the designated amount of
705 time, indicated for each blot separately. The reaction was then quenched by mixing 1:1 with
706 Quench buffer (166 mM Tris-HCl pH 6.8, 10% SDS, 10 mM DTT, 3 µM bromophenol blue,
707 10% glycerol, 100 mM EDTA). These samples were then immediately heated at 90°C for 15
708 minutes, followed by loading onto two 12 or 15% SDS page gels, which were run at 250V for 35

709   minutes. One gel was stained with Coomassie blue, the second was prepared for a Western blot
710   transfer.
711   Filters were soaked in Western blot transfer buffer (25 mM Tris-HCl pH 7.4, 192 mM
712   glycine) supplemented with 0.1% SDS. The membrane was activated in MeOH for 1 minute and
713   then transferred to Western blot transfer buffer supplemented with 20% MeOH. The protein was
714   transferred in a semi-dry apparatus to the membrane at 25 V for one hour. This membrane was
715   then blocked in 5% Carnation non-fat milk powder for one hour while shaking gently. To probe
716   for phospotyrosine, the membrane was then transferred to a 1:2000 dilution of α-phosphotyrosine
717   (Cell Signaling) for shaking overnight at 4°C. The following day, the membrane was washed
718   four times for 10 minutes each in TBS-T (20 mM Tris pH 7.5, 150 mM NaCl, 0.1% Tween-20).
719   The membrane was then transferred to a secondary antibody solution containing a 1:5000
720   dilution of α-mouse HRP (Cell Signaling) for one hour of shaking at room temperature. The
721   membrane was then washed again four times for 10 minutes each in TBS-T. At this point the blot
722   was imaged with Western Bright (Advansta). Blots were quantified using Fiji (ImageJ). For all
723   bands, a local background intensity was measured, and band intensity was calculated as a change
724   in intensity as compared to its local background. For comparison of intensities across replicate
725   blots, average background intensity was calculated for each replicate (based on the local
726   background intensities mentioned above). A scale factor was generated by dividing background
727   intensity of replicate 1 by the average background intensity of replicate 2. The change in
728   intensity for replicate 1 was then divided by the scale factor to ensure that the overall intensity of
729   each blot was consistent. These values are then plotted as "Intensity" for each graph (Figure 3D,
730   4B, 4D, 5C). It should be noted that this technique is only semi-quantitative as the intensity may
731   not be linear with protein concentration, these graphs are provided as a tool to compare trends
732   rather than exact values.
733
734   *Supported-lipid bilayer preparation*
735   Vesicles were prepared by first mixing the desired ratios of PIP$_3$ (Echelon Biosciences,
736   Inc.), 1,2-dioleoyl-sn-glycero-3-[(N-(5-amino-1-carboxypentyl)iminodiacetic acid)succinyl]
737   (nickel salt) (DGS-NTA(Ni)), and 18:1 1,2-dioleoyl-sin-glycero-3-phosphocholine (DOPC)
738   (Avanti Polar Lipids). For experiments with full-length Btk (no His tag) 4% PIP$_3$, 96% DOPC
739   mixtures were prepared. For experiments using His-tagged Btk constructs 4% DGS-NTA(Ni),
740   96% DOPC mixtures were prepared. And for experiments involving LAT 4% PIP$_3$, 4% DGS-
741   NTA(Ni), 92% DOPC bilayers mixtures were prepared. All lipids were stored in solution with
742   chloroform, except PIP$_3$ which was stored in powder form and dissolved in a solution of 1:2:0.8
743   Chloroform:Methanol:Water just before use. After mixing, the solution was dried in an etched 50
744   mL round bottomed flask by rotary evaporation for 15 minutes and then under nitrogen for 15
745   minutes. Dried lipids could then be kept overnight at 4°C, sealed from air or used immediately.
746   The lipids were rehydrated in water to 1 mg/mL lipid concentration by vortexing. Single
747   unilamellar vesicles (SUVs) were created by sonication (Analis Ultrasonic Processor 750 watt,
748   20 kHz) of the lipids at 33% power, 20 seconds on, 50 seconds off for 1 minute 40 seconds of
749   active sonication. A solution of 0.25 mg/mL SUVs in 0.5X TBS was prepared. These were added
750   to a Sticky Slide VI 0.4 (Ibidi GMBH) attached to a Piranha-etched glass slide, 80 μL of SUVs
751   per well. The SUVs were incubated at room temperature for 30 minutes. Each well was then
752   washed with 1 mL of Hepes Buffered Saline (HBS) under vacuum, being careful to avoid
753   introduction of air bubbles to the chamber. When using DGS-NTA(Ni), the wells were then
754   incubated with 100 mM NiCl$_2$ for 5 minutes, and again washed with 1 mL HBS. At this point,

755 the wells were blocked with either 1 µg/mL Poly(L-Lysine)-PEG (PLL-PEG) for 1 minute, or 1
756 mg/mL Bovine Serum Albumin (BSA) or β-Casein for 10 minutes. The blocking agent for each
757 experiment was optimized by checking the mobile fraction of surface bound particles. In the case
758 of full-length Btk on 4% PIP$_3$ bilayers, 1 µg/mL PLL-PEG yielded the best results. For LAT
759 containing bilayers, 1 mg/mL BSA was used to block. For all other experiments, 1 mg/mL β-
760 Casein yielded the best results.
761   For experiments where DGS-NTA(Ni) lipids were used to coordinate His-tagged protein
762 to the bilayers, the protein was added at the desired incubation concentration and left at room
763 temperature for 40 minutes. The chambers were then washed with 600 µL HBS gently by hand
764 and incubated for 20 more minutes at room temperature. They were then again washed with 600
765 µL HBS. Finally, they were washed with 100 µL imaging buffer containing 100 µg/mL BSA or
766 β-Casein (depending on the blocking agent that was used initially) and 10 mM BME in HBS.
767
768 *Monitoring membrane recruitment by fluorescence microscopy*
769   TIRF adsorption experiments were carried out and collected on a Nikon Eclipse Ti-
770 inverted microscope and Andor iXon camera, as described (Bhattacharyya et al., 2020). TIRF
771 data were acquired at 15 second intervals, and data were generally displayed as a difference
772 intensity, where the baseline for a given sample was calculated from the average of the four
773 frames preceding Grb2 addition. Single-molecule traces were recorded as described previously
774 (J. J. Lin et al., 2020). Btk was allowed to equilibrate with the supported-lipid bilayers for 30
775 minutes before imaging. Movies were recorded at intervals of 20 ms, and five or more traces of
776 500-600 frames were collected at various places across the sample. Fluorescent molecules in
777 these movies were tracked using the TrackMate plugin from Fiji (Image J). Tracking parameters
778 were kept consistent across experiments. An immobile fraction of fluorescent Btk was always
779 observed, and this fraction was excluded from the analysis. Tracks were analyzed by calculating
780 a step size distribution and dwell time for the particles, as described in the main text.
781
782 *Reconstitution of LAT phase preparation on supported-lipid bilayers*
783   LAT was reconstituted on supported-lipid bilayers as described (Huang, Ditlev, et al.,
784 2017). Supported-lipid bilayers were prepared as described above with 30 nM His$_6$-Hck and 150
785 nM His$_6$-LAT-Alexa Fluor 555 on a 4% DGS-NTA(Ni), 96% DOPC. The LAT was
786 phosphorylated by including 1 mM ATP and 10 mM MgCl$_2$ in the imaging buffer and incubating
787 for 20 minutes before adding other components. After phosphorylation, the LAT phase transition
788 was induced by adding 6 µM Grb2 and 1.8 µM proline-rich region of SOS (SOS-PRR) and
789 incubated for at least 1 hour. For experiments monitoring Btk diffusion and dwell time, 1 nM Btk
790 T403AzF-Cy5 was also added at this point. After LAT was observed to undergo phase
791 separation, multiple traces of Btk diffusion were recorded and analyzed as described above for
792 single molecule tracking.
793

808   **References**

809   Ahmed, Z., Timsah, Z., Suen, K. M., Cook, N. P., Lee, G. R., Lin, C.-C., … Ladbury, J. E.
810   (2015). Grb2 monomer-dimer equilibrium determines normal versus oncogenic function.
811   *Nature Communications*, *6*, 7354. doi: 10.1038/ncomms8354

812   Amatya, N., Lin, D. Y.-W., & Andreotti, A. H. (2019). Dynamic regulatory features of the
813   protein tyrosine kinases. *Biochemical Society Transactions*, *47*(4), 1101–1116. doi:
814   10.1042/BST20180590

815   Amiram, M., Haimovich, A. D., Fan, C., Wang, Y.-S., Aerni, H.-R., Ntai, I., … Isaacs, F. J.
816   (2015). Evolution of translation machinery in recoded bacteria enables multi-site incorporation
817   of nonstandard amino acids. *Nature Biotechnology*, *33*(12), 1272–1279. doi: 10.1038/nbt.3372

818   Andreotti, A. H., Joseph, R. E., Conley, J. M., Iwasa, J., & Berg, L. J. (2018). Multidomain
819   control over TEC kinase activation state tunes the T cell response. *Annual Review of*
820   *Immunology*, *36*, 549–578. doi: 10.1146/annurev-immunol-042617-053344

821   Baraldi, E., Djinovic Carugo, K., Hyvönen, M., Surdo, P. L., Riley, A. M., Potter, B. V., …
822   Saraste, M. (1999). Structure of the PH domain from Bruton's tyrosine kinase in complex with
823   inositol 1,3,4,5-tetrakisphosphate. *Structure*, *7*(4), 449–460. doi: 10.1016/s0969-
824   2126(99)80057-4

825   Bard, J. A. M., Bashore, C., Dong, K. C., & Martin, A. (2019). The 26S proteasome utilizes a
826   kinetic gateway to prioritize substrate degradation. *Cell*, *177*(2), 286-298.e15. doi:
827   10.1016/j.cell.2019.02.031

828   Bard, J. A. M., & Martin, A. (2018). Recombinant Expression, Unnatural Amino Acid
829   Incorporation, and Site-Specific Labeling of 26S Proteasomal Subcomplexes. *Methods in*
830   *Molecular Biology*, *1844*, 219–236. doi: 10.1007/978-1-4939-8706-1_15

831   Bhattacharyya, M., Lee, Y. K., Muratcioglu, S., Qiu, B., Nyayapati, P., Schulman, H., …
832   Kuriyan, J. (2020). Flexible linkers in CaMKII control the balance between activating and
833   inhibitory autophosphorylation. *ELife*, *9*. doi: 10.7554/eLife.53670

834   Cantor, A. J., Shah, N. H., & Kuriyan, J. (2018). Deep mutational analysis reveals functional
835   trade-offs in the sequences of EGFR autophosphorylation sites. *Proceedings of the National*

Academy of Sciences of the United States of America, *115*(31), E7303–E7312. doi: 10.1073/pnas.1803598115

Chatterjee, A., Sun, S. B., Furman, J. L., Xiao, H., & Schultz, P. G. (2013). A versatile platform for single- and multiple-unnatural amino acid mutagenesis in Escherichia coli. *Biochemistry*, *52*(10), 1828–1837. doi: 10.1021/bi4000244

Chin, J. W., Santoro, S. W., Martin, A. B., King, D. S., Wang, L., & Schultz, P. G. (2002). Addition of p-azido-L-phenylalanine to the genetic code of Escherichia coli. *Journal of the American Chemical Society*, *124*(31), 9026–9027. doi: 10.1021/ja027007w

Chiu, C. W., Dalton, M., Ishiai, M., Kurosaki, T., & Chan, A. C. (2002). BLNK: molecular scaffolding through 'cis'-mediated organization of signaling proteins. *The EMBO Journal*, *21*(23), 6461–6472. doi: 10.1093/emboj/cdf658

Chung, J. K., Lee, Y. K., Denson, J.-P., Gillette, W. K., Alvarez, S., Stephen, A. G., & Groves, J. T. (2018). K-Ras4B Remains Monomeric on Membranes over a Wide Range of Surface Densities and Lipid Compositions. *Biophysical Journal*, *114*(1), 137–145. doi: 10.1016/j.bpj.2017.10.042

Chung, J. K., Nocka, L. M., Decker, A., Wang, Q., Kadlecek, T. A., Weiss, A., … Groves, J. T. (2019). Switch-like activation of Bruton's tyrosine kinase by membrane-mediated dimerization. *Proceedings of the National Academy of Sciences of the United States of America*, *116*(22), 10798–10803. doi: 10.1073/pnas.1819309116

Clark, S. G., Stern, M. J., & Horvitz, H. R. (1992). C. elegans cell-signalling gene sem-5 encodes a protein with SH2 and SH3 domains. *Nature*, *356*(6367), 340–344. doi: 10.1038/356340a0

Courtney, A. H., Lo, W.-L., & Weiss, A. (2018). TCR signaling: mechanisms of initiation and propagation. *Trends in Biochemical Sciences*, *43*(2), 108–123. doi: 10.1016/j.tibs.2017.11.008

Devkota, S., Joseph, R. E., Boyken, S. E., Fulton, D. B., & Andreotti, A. H. (2017). An Autoinhibitory Role for the Pleckstrin Homology Domain of Interleukin-2-Inducible Tyrosine Kinase and Its Interplay with Canonical Phospholipid Recognition. *Biochemistry*, *56*(23), 2938–2949. doi: 10.1021/acs.biochem.6b01182

Duarte, D. P., Lamontanara, A. J., La Sala, G., Jeong, S., Sohn, Y.-K., Panjkovich, A., … Hantschel, O. (2020). Btk SH2-kinase interface is critical for allosteric kinase activation and its targeting inhibits B-cell neoplasms. *Nature Communications*, *11*(1), 2319. doi: 10.1038/s41467-020-16128-5

Engels, N., Engelke, M., & Wienands, J. (2008). *Conformational Plasticity and Navigation of Signaling Proteins in Antigen-Activated B Lymphocytes*. In *Advances in Immunology*: *Vol. 97* (pp. 251–281). Elsevier. doi: 10.1016/S0065-2776(08)00005-9

870 Engels, N., König, L. M., Heemann, C., Lutz, J., Tsubata, T., Griep, S., … Wienands, J. (2009).
871   Recruitment of the cytoplasmic adaptor Grb2 to surface IgG and IgE provides antigen
872   receptor-intrinsic costimulation to class-switched B cells. *Nature Immunology*, *10*(9), 1018–
873   1025. doi: 10.1038/ni.1764

874 Engels, N., König, L. M., Schulze, W., Radtke, D., Vanshylla, K., Lutz, J., … Wienands, J.
875   (2014). The immunoglobulin tail tyrosine motif upgrades memory-type BCRs by
876   incorporating a Grb2-Btk signalling module. *Nature Communications*, *5*, 5456. doi:
877   10.1038/ncomms6456

878 Gale, N. W., Kaplan, S., Lowenstein, E. J., Schlessinger, J., & Bar-Sagi, D. (1993). Grb2
879   mediates the EGF-dependent activation of guanine nucleotide exchange on Ras. *Nature*,
880   *363*(6424), 88–92. doi: 10.1038/363088a0

881 Ganti, R. S., Lo, W.-L., McAffee, D. B., Groves, J. T., Weiss, A., & Chakraborty, A. K. (2020).
882   How the T cell signaling network processes information to discriminate between self and
883   agonist ligands. *Proceedings of the National Academy of Sciences of the United States of*
884   *America*, *117*(42), 26020–26030. doi: 10.1073/pnas.2008303117

885 Hantschel, O., Nagar, B., Guettler, S., Kretzschmar, J., Dorey, K., Kuriyan, J., & Superti-Furga,
886   G. (2003). A myristoyl/phosphotyrosine switch regulates c-Abl. *Cell*, *112*(6), 845–857. doi:
887   10.1016/s0092-8674(03)00191-0

888 Hashimoto, S., Iwamatsu, A., Ishiai, M., Okawa, K., Yamadori, T., Matsushita, M., … Tsukada,
889   S. (1999). Identification of the SH2 domain binding protein of Bruton's tyrosine kinase as
890   BLNK--functional significance of Btk-SH2 domain in B-cell antigen receptor-coupled
891   calcium signaling. *Blood*, *94*(7), 2357–2364.

892 Hein, M. Y., Hubner, N. C., Poser, I., Cox, J., Nagaraj, N., Toyoda, Y., … Mann, M. (2015). A
893   human interactome in three quantitative dimensions organized by stoichiometries and
894   abundances. *Cell*, *163*(3), 712–723. doi: 10.1016/j.cell.2015.09.053

895 Hendriks, R. W., Yuvaraj, S., & Kil, L. P. (2014). Targeting Bruton's tyrosine kinase in B cell
896   malignancies. *Nature Reviews. Cancer*, *14*(4), 219–232. doi: 10.1038/nrc3702

897 Huang, W. Y. C., Alvarez, S., Kondo, Y., Lee, Y. K., Chung, J. K., Lam, H. Y. M., … Groves, J.
898   T. (2019). A molecular assembly phase transition and kinetic proofreading modulate Ras
899   activation by SOS. *Science*, *363*(6431), 1098–1103. doi: 10.1126/science.aau5721

900 Huang, W. Y. C., Chiang, H.-K., & Groves, J. T. (2017). Dynamic Scaling Analysis of
901   Molecular Motion within the LAT:Grb2:SOS Protein Network on Membranes. *Biophysical*
902   *Journal*, *113*(8), 1807–1813. doi: 10.1016/j.bpj.2017.08.024

903 Huang, W. Y. C., Ditlev, J. A., Chiang, H.-K., Rosen, M. K., & Groves, J. T. (2017). Allosteric
904   modulation of grb2 recruitment to the intrinsically disordered scaffold protein, LAT, by

905   remote site phosphorylation. *Journal of the American Chemical Society*, *139*(49), 18009–
906   18015. doi: 10.1021/jacs.7b09387

907 Huang, W. Y. C., Yan, Q., Lin, W.-C., Chung, J. K., Hansen, S. D., Christensen, S. M., …
908   Groves, J. T. (2016). Phosphotyrosine-mediated LAT assembly on membranes drives kinetic
909   bifurcation in recruitment dynamics of the Ras activator SOS. *Proceedings of the National*
910   *Academy of Sciences of the United States of America*, *113*(29), 8218–8223. doi:
911   10.1073/pnas.1602602113

912 Hyvönen, M., & Saraste, M. (1997). Structure of the PH domain and Btk motif from Bruton's
913   tyrosine kinase: molecular explanations for X-linked agammaglobulinaemia. *The EMBO*
914   *Journal*, *16*(12), 3396–3404. doi: 10.1093/emboj/16.12.3396

915 Joseph, R. E., Wales, T. E., Fulton, D. B., Engen, J. R., & Andreotti, A. H. (2017). Achieving a
916   graded immune response: BTK adopts a range of active/inactive conformations dictated by
917   multiple interdomain contacts. *Structure*, *25*(10), 1481-1494.e4. doi: 10.1016/j.str.2017.07.014

918 Kaizuka, Y., & Groves, J. T. (2004). Structure and dynamics of supported intermembrane
919   junctions. *Biophysical Journal*, *86*(2), 905–912. doi: 10.1016/S0006-3495(04)74166-1

920 Kim, W., Kim, E., Min, H., Kim, M. G., Eisenbeis, V. B., Dutta, A. K., … Seong, R. H. (2019).
921   Inositol polyphosphates promote T cell-independent humoral immunity via the regulation of
922   Bruton's tyrosine kinase. *Proceedings of the National Academy of Sciences of the United*
923   *States of America*, *116*(26), 12952–12957. doi: 10.1073/pnas.1821552116

924 Knight, J. D., & Falke, J. J. (2009). Single-molecule fluorescence studies of a PH domain: new
925   insights into the membrane docking reaction. *Biophysical Journal*, *96*(2), 566–582. doi:
926   10.1016/j.bpj.2008.10.020

927 Koretzky, G. A., Abtahian, F., & Silverman, M. A. (2006). SLP76 and SLP65: complex
928   regulation of signalling in lymphocytes and beyond. *Nature Reviews. Immunology*, *6*(1), 67–
929   78. doi: 10.1038/nri1750

930 Kurosaki, T., & Tsukada, S. (2000). BLNK: connecting Syk and Btk to calcium signals.
931   *Immunity*, *12*(1), 1–5. doi: 10.1016/s1074-7613(00)80153-3

932 Lander, G. C., Estrin, E., Matyskiela, M. E., Bashore, C., Nogales, E., & Martin, A. (2012).
933   Complete subunit architecture of the proteasome regulatory particle. *Nature*, *482*(7384), 186–
934   191. doi: 10.1038/nature10774

935 Lin, C.-C., Melo, F. A., Ghosh, R., Suen, K. M., Stagg, L. J., Kirkpatrick, J., … Ladbury, J. E.
936   (2012). Inhibition of basal FGF receptor signaling by dimeric Grb2. *Cell*, *149*(7), 1514–1524.
937   doi: 10.1016/j.cell.2012.04.033

938   Lin, C.-W., Nocka, L. M., Stinger, B., DeGrandchamp, J., Lew, N., Alvarez, S., … Groves, J. T.
939   (2021). A two-component protein condensate of EGFR and Grb2 regulates Ras activation at
940   the membrane. *BioRxiv*. doi: 10.1101/2021.12.12.472247

941   Lin, C.-W., Nocka, L. M., Stinger, B. L., DeGrandchamp, J. B., Lew, L. J. N., Alvarez, S., …
942   Groves, J. T. (2022). A two-component protein condensate of the EGFR cytoplasmic tail and
943   Grb2 regulates Ras activation by SOS at the membrane. *Proceedings of the National Academy*
944   *of Sciences of the United States of America*, *119*(19), e2122531119. doi:
945   10.1073/pnas.2122531119

946   Lin, J. J., O'Donoghue, G. P., Wilhelm, K. B., Coyle, M. P., Low-Nam, S. T., Fay, N. C., …
947   Groves, J. T. (2020). Membrane Association Transforms an Inert Anti-TCRβ Fab' Ligand into
948   a Potent T Cell Receptor Agonist. *Biophysical Journal*, *118*(12), 2879–2893. doi:
949   10.1016/j.bpj.2020.04.018

950   Liu, S. K., Fang, N., Koretzky, G. A., & McGlade, C. J. (1999). The hematopoietic-specific
951   adaptor protein gads functions in T-cell signaling via interactions with the SLP-76 and LAT
952   adaptors. *Current Biology*, *9*(2), 67–75. doi: 10.1016/s0960-9822(99)80017-7

953   Lowenstein, E. J., Daly, R. J., Batzer, A. G., Li, W., Margolis, B., Lammers, R., … Schlessinger,
954   J. (1992). The SH2 and SH3 domain-containing protein GRB2 links receptor tyrosine kinases
955   to ras signaling. *Cell*, *70*(3), 431–442. doi: 10.1016/0092-8674(92)90167-b

956   Maignan, S., Guilloteau, J. P., Fromage, N., Arnoux, B., Becquart, J., & Ducruix, A. (1995).
957   Crystal structure of the mammalian Grb2 adaptor. *Science*, *268*(5208), 291–293. doi:
958   10.1126/science.7716522

959   Mayer, B. J., Jackson, P. K., Van Etten, R. A., & Baltimore, D. (1992). Point mutations in the abl
960   SH2 domain coordinately impair phosphotyrosine binding in vitro and transforming activity in
961   vivo. *Molecular and Cellular Biology*, *12*(2), 609–618. doi: 10.1128/mcb.12.2.609-618.1992

962   Moarefi, I., LaFevre-Bernt, M., Sicheri, F., Huse, M., Lee, C. H., Kuriyan, J., & Miller, W. T.
963   (1997). Activation of the Src-family tyrosine kinase Hck by SH3 domain displacement.
964   *Nature*, *385*(6617), 650–653. doi: 10.1038/385650a0

965   Moroco, J. A., Craigo, J. K., Iacob, R. E., Wales, T. E., Engen, J. R., & Smithgall, T. E. (2014).
966   Differential sensitivity of Src-family kinases to activation by SH3 domain displacement. *Plos*
967   *One*, *9*(8), e105629. doi: 10.1371/journal.pone.0105629

968   Nagar, B., Hantschel, O., Young, M. A., Scheffzek, K., Veach, D., Bornmann, W., … Kuriyan, J.
969   (2003). Structural basis for the autoinhibition of c-Abl tyrosine kinase. *Cell*, *112*(6), 859–871.
970   doi: 10.1016/s0092-8674(03)00194-6

971   Nye, J. A., & Groves, J. T. (2008). Kinetic control of histidine-tagged protein surface density on
972   supported lipid bilayers. *Langmuir: The ACS Journal of Surfaces and Colloids*, *24*(8), 4145–
973   4149. doi: 10.1021/la703788h

974 Olivier, J. P., Raabe, T., Henkemeyer, M., Dickson, B., Mbamalu, G., Margolis, B., … Pawson,
975   T. (1993). A Drosophila SH2-SH3 adaptor protein implicated in coupling the sevenless
976   tyrosine kinase to an activator of Ras guanine nucleotide exchange, Sos. *Cell*, *73*(1), 179–191.
977   doi: 10.1016/0092-8674(93)90170-u

978 Ozdener, F., Dangelmaier, C., Ashby, B., Kunapuli, S. P., & Daniel, J. L. (2002). Activation of
979   phospholipase Cgamma2 by tyrosine phosphorylation. *Molecular Pharmacology*, *62*(3), 672–
980   679. doi: 10.1124/mol.62.3.672

981 Reif, K., Buday, L., Downward, J., & Cantrell, D. A. (1994). SH3 domains of the adapter
982   molecule Grb2 complex with two proteins in T cells: the guanine nucleotide exchange protein
983   Sos and a 75-kDa protein that is a substrate for T cell antigen receptor-activated tyrosine
984   kinases. *The Journal of Biological Chemistry*, *269*(19), 14081–14087.

985 Rip, J., Van Der Ploeg, E. K., Hendriks, R. W., & Corneth, O. B. J. (2018). The role of bruton's
986   tyrosine kinase in immune cell signaling and systemic autoimmunity. *Critical Reviews in
987   Immunology*, *38*(1), 17–62. doi: 10.1615/CritRevImmunol.2018025184

988 Rodriguez, R., Matsuda, M., Perisic, O., Bravo, J., Paul, A., Jones, N. P., … Katan, M. (2001).
989   Tyrosine residues in phospholipase Cgamma 2 essential for the enzyme function in B-cell
990   signaling. *The Journal of Biological Chemistry*, *276*(51), 47982–47992. doi:
991   10.1074/jbc.M107577200

992 Scharenberg, A. M., Humphries, L. A., & Rawlings, D. J. (2007). Calcium signalling and cell-
993   fate choice in B cells. *Nature Reviews. Immunology*, *7*(10), 778–789. doi: 10.1038/nri2172

994 Seeliger, M. A., Young, M., Henderson, M. N., Pellicena, P., King, D. S., Falick, A. M., &
995   Kuriyan, J. (2005). High yield bacterial expression of active c-Abl and c-Src tyrosine kinases.
996   *Protein Science*, *14*(12), 3135–3139. doi: 10.1110/ps.051750905

997 Shah, N. H., Amacher, J. F., Nocka, L. M., & Kuriyan, J. (2018). The Src module: an ancient
998   scaffold in the evolution of cytoplasmic tyrosine kinases. *Critical Reviews in Biochemistry
999   and Molecular Biology*, *53*(5), 535–563. doi: 10.1080/10409238.2018.1495173

1000 Shi, T., Niepel, M., McDermott, J. E., Gao, Y., Nicora, C. D., Chrisler, W. B., … Wiley, H. S.
1001   (2016). Conservation of protein abundance patterns reveals the regulatory architecture of the
1002   EGFR-MAPK pathway. *Science Signaling*, *9*(436), rs6. doi: 10.1126/scisignal.aaf0891

1003 Su, X., Ditlev, J. A., Hui, E., Xing, W., Banjade, S., Okrut, J., … Vale, R. D. (2016). Phase
1004   separation of signaling molecules promotes T cell receptor signal transduction. *Science*,
1005   *352*(6285), 595–599. doi: 10.1126/science.aad9964

1006 Tsukada, S., Saffran, D. C., Rawlings, D. J., Parolini, O., Allen, R. C., Klisak, I., … Quan, S.
1007   (1993). Deficient expression of a B cell cytoplasmic tyrosine kinase in human X-linked
1008   agammaglobulinemia. *Cell*, *72*(2), 279–290. doi: 10.1016/0092-8674(93)90667-f

1009   Wang, Q., Pechersky, Y., Sagawa, S., Pan, A. C., & Shaw, D. E. (2019). Structural mechanism
1010   for Bruton's tyrosine kinase activation at the cell membrane. *Proceedings of the National*
1011   *Academy of Sciences of the United States of America*, *116*(19), 9390–9399. doi:
1012   10.1073/pnas.1819301116

1013   Wang, Q., Vogan, E. M., Nocka, L. M., Rosen, C. E., Zorn, J. A., Harrison, S. C., & Kuriyan, J.
1014   (2015). Autoinhibition of Bruton's tyrosine kinase (Btk) and activation by soluble inositol
1015   hexakisphosphate. *ELife*, *4*, e06074. doi: 10.7554/eLife.06074

1016   Weiss, A., & Littman, D. R. (1994). Signal transduction by lymphocyte antigen receptors. *Cell*,
1017   *76*(2), 263–274. doi: 10.1016/0092-8674(94)90334-4

1018   Yeung, W., Kwon, A., Taujale, R., Bunn, C., Venkat, A., & Kannan, N. (2021). Evolution of
1019   functional diversity in the holozoan tyrosine kinome. *Molecular Biology and Evolution*,
1020   *38*(12), 5625–5639. doi: 10.1093/molbev/msab272